M 2017

U. PORTO
FEUP FACULDADE DE ENGENHARIA
UNIVERSIDADE DO PORTO

TEST METHOD DEVELOPMENT TO ASSESS THE ADHESION OF TIRE REINFORCEMENTS TO RUBBER UNDER DYNAMIC CONDITIONS

DANIEL DE CASTRO PINHO
DISSERTAÇÃO DE MESTRADO APRESENTADA
À FACULDADE DE ENGENHARIA DA UNIVERSIDADE DO PORTO EM
ÁREA CIENTÍFICA

Mestrado Integrado em Engenharia Química

Test Method development to assess the adhesion of tire reinforcements to rubber under dynamic conditions

Master Thesis

by

Daniel de Castro Pinho

Performed at

Continental AG - Body Compound & Reinforcement Technology Department

Supervisor at FEUP: **Prof. Fernão Magalhães**

Supervisor at Continental: **Dr. Thomas Kramer**

Universidade do Porto
Faculdade de Engenharia
FEUP

Departamento de Engenharia Química

February of 2017

Acknowledgements

After performing this master thesis in Hannover, I had the opportunity to meet many people that ended up motivating me to achieve the best possible experience, both personally and professionally.

This work would not be possible without the help of Dr. Thomas Kramer. I wish to express my gratitude for such remarkable support, availability, encouraging words, hints and patience, but most and foremost, for allowing me to have this chance to realize how promising chemical engineering can be.

To Professor Fernão Magalhães, I want to thank for all the support provided and also for understanding all the limitations, the unexpected changes throughout the internship and the work rhythm.

I would like to highlight all the crucial help I received both from Christian Neufeld and Tiago Moura, as well as all the people from the Reinforcement Testing Laboratory. Furthermore, I would like to thank Viktoria Werner for the conceded opportunity to perform this mater thesis abroad.

To Diana Gomes, Ricardo Protásio and Raza Haider, thank you for our conversations, all your help, all the motivation you gave me and all the support throughout this internship.

To Goncalo Ferraz, I will always be grateful for your help since day one.

To my best friends, José, Bruno, Gonçalo and Jhonny, you just proved that no matter where we are, or the distance that is between us, I can always count with your support.

To my parents and my brother, as well as the entire family, I have to thank for making these months abroad a lot easier. Despite all the distance, I felt like home, and all of you know how important every conversation was, to overcome every daily challenge. There will never be enough words to describe how lucky I am for having you all. Thank you very much for everything.

Resumo

O objetivo principal desta tese de mestrado foi o estudo da adesão dos materiais de reforço utilizados em pneus atuais. Dependendo dos materiais a serem testados, diferentes métodos são utilizados. O *3 Cord Adhesion Test* permitiu avaliar a adesão entre borracha e cordas de aço. O *Oldy Test*, possibilitou avaliar a adesão entre borracha e cordas têxteis com diferentes promotores de adesão.

Quanto ao *3 Cord Adhesion Test*, o foco foi melhorar o método de teste usado pela Continental, através da realização de ensaios, de modo a perceber quais os parâmetros que influenciam os resultados obtidos, aquando da medição da força para remover cordas de aço das amostras de borracha.

Assim sendo, não só foram tidos em conta fatores como a orientação da amostra, bem como a respetiva simetria, mas também, foi estabelecido um tempo de espera de 48 a 72 horas, entre a vulcanização e o início do procedimento de teste. Para além disso, no decorrer do estágio, foi possível implementar uma nova configuração nas amostras a testar.

Relativamente à realização de condições dinâmicas, e tendo em consideração a importância das mesmas para a indústria, devido ao facto de permitirem uma melhor simulação da condição de serviço do pneu, o *Oldy Test* permitiu a avaliação de diferentes promotores de adesão para os têxteis compostos por Híbrido, Nylon e Poliéster.

Dos dois promotores de adesão testados para o Híbrido, os melhores resultados foram obtidos para H1, sendo a média obtida 44874.00 ciclos e um desvio padrão de ± 4623.86 ciclos. Para o Nylon, o melhor promotor de adesão foi N5, tendo sido obtida uma média de 375136.40 ciclos e um desvio padrão de ± 52700.85 ciclos.

Relativamente ao Poliéster, o maior número de ciclos foi obtido por P2, sendo a média de ciclos 48565.00 e o desvio padrão ± 4610.80 ciclos.

Palavras Chave: adesão, ensaio dinâmico, promotores de adesão, reforços de aço, reforços têxteis;

Abstract

The main goal of this master thesis was to study the adhesion of reinforcement materials used on current tires. Depending on the materials in need to be tested, different test methods are developed. The 3 Cord Adhesion Test allowed for the evaluation of the adhesion between rubber and steel cords. The Oldy Test, allowed for the evaluation of the adhesion between rubber and textile cords with different adhesion promoters.

For the 3 Cord Adhesion Test, the focus was to improve the test method used by Continental, alongside with the performance of tests to better understand which parameters have an influence on the results, while measuring the force to peel steel cords from the rubber samples.

Hence, not only factors such as the orientation of the sample, as well as its symmetry, were employed, but also, the definition of a waiting period between vulcanization and the testing of the samples, was established from 48 to 72 hours. Furthermore, throughout the internship, it was possible to implement a new configuration for the samples being tested.

Regarding the performance of dynamic conditions, and taking into account its importance to the industry, due to the fact that they allow for a better simulation of the service condition of the tire, the Oldy Test was performed to evaluate different adhesion promoters for Hybrid, Nylon and Polyester textiles.

From the two adhesion promoters tested for the Hybrid, the best results were obtained from H1, with an average of 44874.00 cycles, and a standard deviation of ± 4623.86 cycles. For the Nylon, the best adhesion promoter was N5, reaching an average of 375136.40 cycles and a standard deviation of ± 52700.85 cycles. Regarding the Polyester, the best adhesion promoter achieved an average of 48565.00 cycles and its standard deviation was ± 4610.80 cycles.

Keywords: adhesion, dynamic test, adhesion promoters, steel reinforcement, textile reinforcement;

Official Statement

I declare, under honor of commitment, that the present work is original and that every non original contribution was properly referred by identifying its source.

Signature and date

Index

Notation and Glossary

List of Variables

A	*Amplitude*	*mm*
F	*Force/Load*	*N*
T	*Temperature*	*ºC*
S	*Strain*	*mm*
f	*Frequency*	*Hz*

1 Introduction

1.1 Project presentation and framework

Taking into account all the technology available nowadays, and combining it with the know-how developed over the decades, it is expected that in order to improve the features of current tires, the available test methods gain more and more importance.

As a result, to enhance all the materials used in tires, to better understand their properties, and in order to better perceive their behavior when in contact with each other, the need of systematic investigations is justified. With this master thesis, the focus was placed on the reinforcement materials, due to its importance when implemented on the tire. Its advantages are innumerous as a consequence of the bonds between the reinforcing cords and the elastomers, especially on the carcass and the belt.

With this master thesis, the goal was to go over two test methods capable of studying the adhesion systems between rubber and steel cords, as well as, between rubber and textile cords. Both test methods are promising regarding the possibility of performing both static and dynamic tests, being the latest essential to the industry, due to the fact that they allow a better simulation of the service condition of the tire, although, these are highly time consuming and costly.

1.2 Continental AG

Continental was founded in Hanover in 1871 as the stock corporation “Continental-Caoutchouc- und Gutta-Percha Compagnie”. Manufacturing at the main factory in Hanover included soft rubber products, rubberized fabrics, and solid tires for carriages and bicycles [1].

Currently, Continental ranks among the top 5 automotive suppliers worldwide. As a supplier of brake systems, systems and components for powertrains and chassis, instrumentation, infotainment solutions, vehicle electronics, tires and technical elastomers, Continental contributes to enhanced driving safety and global climate protection. Continental is also a competent partner in networked automobile communication [1].

In order to better understand the fields in which Continental is present, as well as its magnitude, additional information is presented in *Figure 1*.

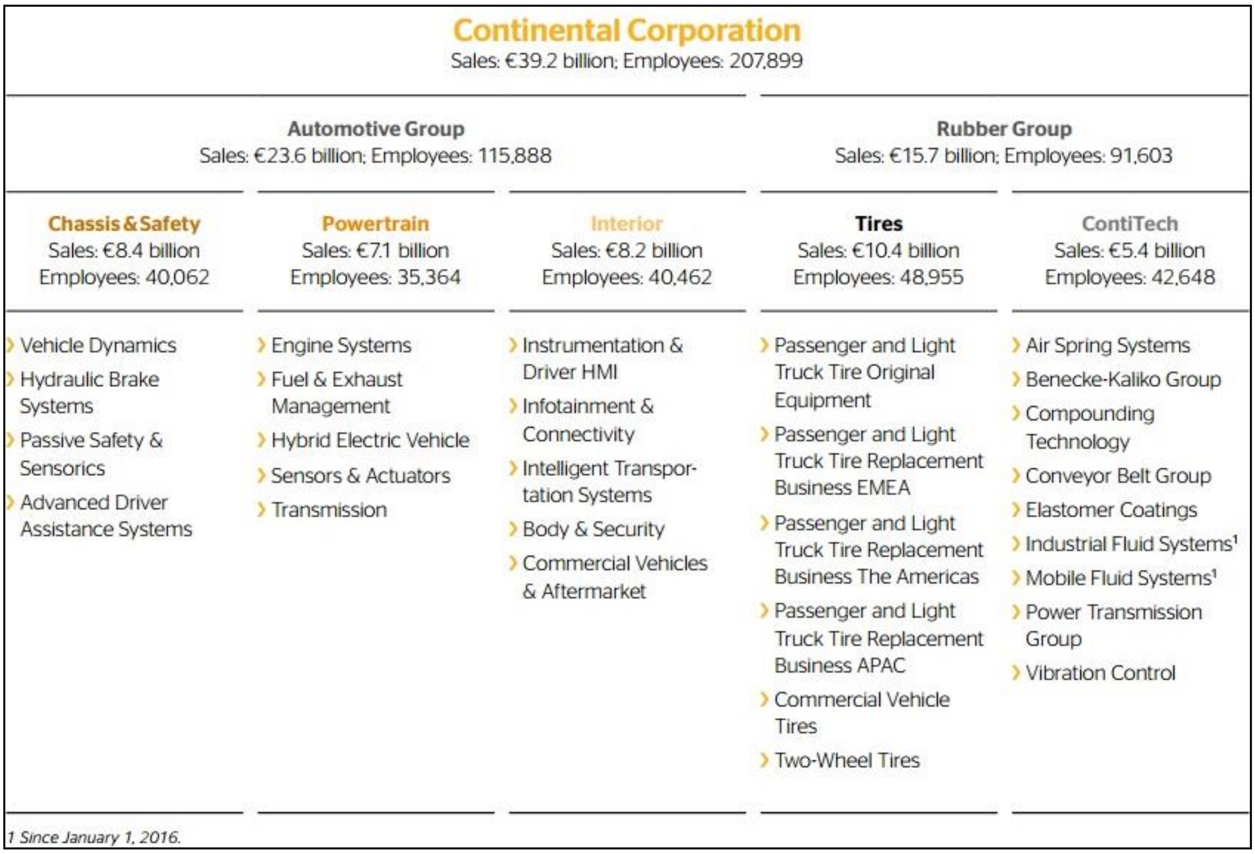

Figure 1 – Structure of the Continental Corporation [2]

1.3 Work goals and contributions

The purpose of this master thesis was the development of two test methods capable to perform both static and dynamic tests, in order to test the performance of adhesion systems involved in the reinforcement of tires.

For the first test method, the 3 Cord Adhesion Test, the goal was to assess the adhesion between rubber and steel cords. Since preliminary studies revealed irregular results on every sample, the focus was to go over all the possible factors causing this behavior, in order to improve the current test method and the testing conditions.

The second test method, Oldy Test, allowed to compare not only the behavior of the samples, but also, the adhesion between rubber and textile cords with different adhesion promoters: Hybrid, Nylon and Polyester.

1.4 Thesis organization

The content of this master thesis is divided in 6 chapters. The description of each chapter is mentioned below:

Chapter 1: Introduction. In this section, the goal is to present the need of this work for the company, as well as to provide a brief introduction of Continental.

Chapter 2: State of the Art. The main aspects concerning the tire, its materials, the role of reinforcement and its importance.

Chapter 3: Test Development Description and Discussion. All the technology and the test methods used during the internship are presented.

Chapter 4: Results and Test Method Validation. Allows for the analysis of all the results obtained for both test methods.

Chapter 5: Conclusions. The focus is to highlight the main results of this master thesis.

Chapter 6: Project Assessment. Critical approach of the developed work, its limitations and suggestions to implement in future studies.

2 State of the art

2.1 Tire Overview

The tire is a complex technical component of today's motor cars and must perform a variety of functions. It must cushion, dampen, assure good directional stability, and provide long term service [2].

Most and foremost, a tire must be capable of transmitting strong longitudinal and lateral forces (during breaking, acceleration and cornering maneuvers) in order to assure optimal and reliable roadholding quality [2]. Regardless of the environment, it is expected that the performance can be the closest to the ideal, assuring the highest safety levels, providing the best driving experience.

As far as evolution is concerned, over the past 5,000 years it was necessary to reinvent it in order to meet the desired needs in different locations. However, the greatest technological advancements took place since the last decades of the 19th century.

As far as Continental innovation is concerned, in 1898 the brand started producing the so called "pneumatics". These tires, were capable of giving a more comfortable ride and enabling automobiles to travel at higher speeds [2].

Features such as the tread pattern, the black color, the addition of carbon black resulting in an increase of tires' toughness and durability, as well as the low pressure tire (or "balloon") were some of the most important achievements reached during the first half of the 20th century.

Nowadays, modern passenger cars radials are composed up to 25 different structural parts and as many as 12 different rubber compounds. The main structural elements are the casing and the tread/belt assembly. The casing cushions the tire and contains the required volume of air. The tread/belt assembly envelops the casing and provides for low rolling resistance, optimum driving behavior and good mileage [2].

2.1.1 Cross Ply Tires vs Modern Radial Tire

The tires used currently, radial – or belted – tires, have completely replaced the cross –ply tires mainly used until 1970, *Figure 2*. The cords in a radial tire casing run perpendicular to the direction of travel, as can be seen in Figure 3. Viewed from the side, the cords run radially – giving the tire its name.

The weakness of this arrangement is that the cords cannot sufficiently absorb lateral forces when cornering or circumferential forces when accelerating, *Figure 3*. To compensate this, the cords must be supported or complemented by other structural elements.

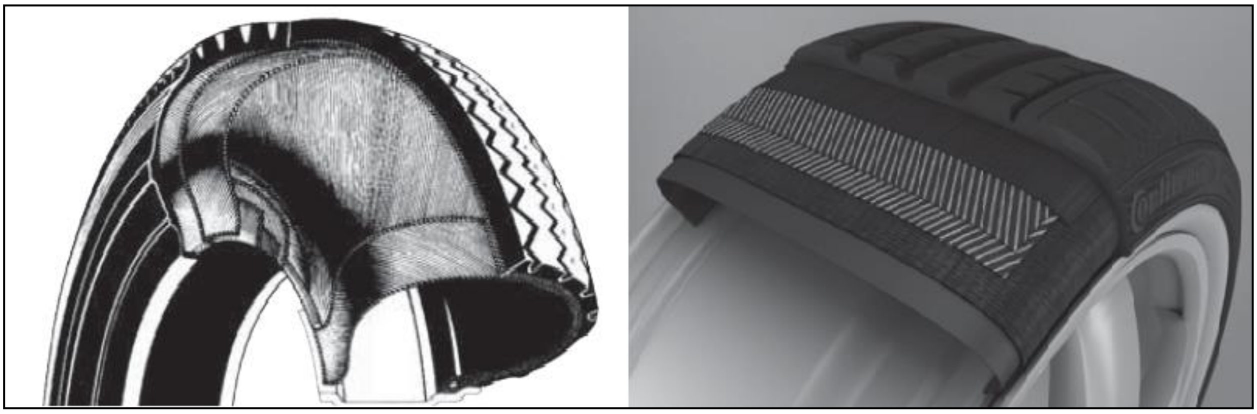

Figure 2- Cross-Ply Tire (left) vs Radial Tire (right) (Adapted from (2))

The belt assembly comprises several layers of steel belt plies arranged in diagonally opposing directions at a specified angle. The belt assembly provides support and stability to the tread area so that the forces in the 3 principal planes can be transmitted efficiently. Many tires are additionally stabilized by a nylon cap ply.

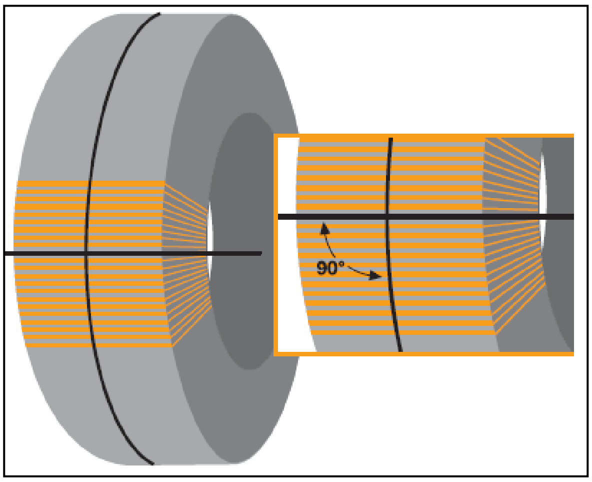

Figure 3 – Radial Tire Structure [2]

On the other hand, the casing of a cross-ply tire consisted of a number of rubberized cord plies with edges wrapped around the bead wire (the bead ensures that the tire sits firmly on the rim). The number of plies determines the load capacity of the tire. Cross-ply tires for passenger cars generally had between two and six rayon or nylon cord plies. The individual cord plies of a cross-ply tire are arranged in a criss-cross pattern at a certain angle– known as the cord angle. This angle determines the tire's characteristics [2].

2.2 Materials used in a tire

In order to produce a tire, it is necessary to conjugate a diversity of materials in different amounts, depending not only on the intended purpose, but also on factors such as the size and the climate. Usually, the used materials are listed used as follows, and as shown in *Figure 4* [2]:

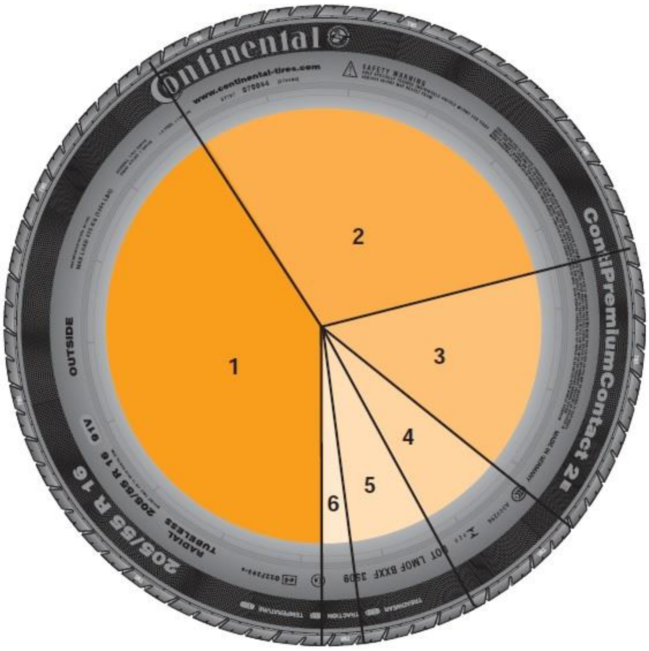

Figure 4 – Breakdown of ingredients [2]

1- Rubber (natural and synthetic rubber). 41%

2- Fillers (carbon black, silica, carbon, chalk). 30%

3- Reinforcement materials (steel, polyester, rayon, nylon). 15%

4- Plasticizers (oils and resins). 6%

5- Chemicals for vulcanization (sulphur, zinc oxide, various other chemicals). 6%

6- Anti-ageing agents and other chemicals. 2%

2.3 Tire Components

After considering the materials used in a tire, it is important to realize where they are applied and how they are distributed, *Figure 5*. Taking into account the complexity of the resulting structure, a segmented and detailed explanation of its functions is necessary.

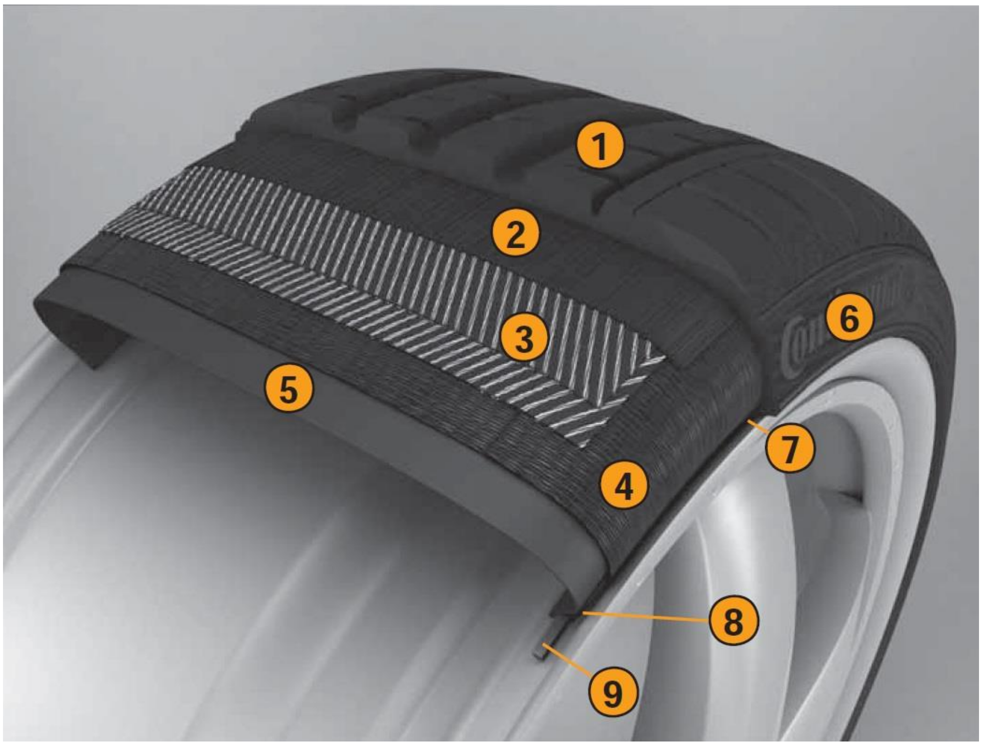

Figure 5 – Radial Tire Structure [2]

A modern tire is made up of [2]:

➢ Tread/belt assembly consisting of:

1- Tread – ensures high mileage, good road grip and water expulsion. Mainly composed out of synthetic and natural rubber. It is divided as follows:

✓ Cap: provides grip on all road surfaces, wear-resistance and directional stability.

✓ Base: reduces rolling resistance and damage to the casing.

✓ Shoulder: forms an optimal transition from the tread to the sidewall.

2- Jointless cap plies – enable high speeds. Consists in nylon embedded in rubber.

3- Steel-cord belt plies – optimize directional stability and rolling resistance. Furthermore, it enhances shape retention and directional stability, it reduces the rolling resistance and it increases the tire's mileage performance.

- Casing, consisting of:

4- Textile cord ply – controls internal pressure and maintains the tire's shape. It is made out of rayon or polyester (rubberized).

5- Inner liner – makes the tire airtight. It seals the air-filled inner chamber and it acts as a tube in tubeless tires. Butyl rubber is the selected material for this component.

6- Side wall – protects from external damage and atmospheric conditions. It is built using natural rubber.

7- Bead reinforcement – promotes directional stability and precise steering response. Made of nylon and aramid.

8- Bead apex – promotes directional stability, steering performance and comfort level. Composed by synthetic rubber.

9- Bead core – ensures firm seating on the rim, as a result of steel wire embedded in rubber.

2.4 Tire Reinforcement Materials

Due to the fact that many elastomers used in tires do not provide enough strength, it is necessary to implement materials capable of improving the overall properties, in order to reinforce the system. A list of the main materials is presented, as well as its applications, advantages and disadvantages [3]:

<u>Nylon</u>: type 6 and 6,6 tire cords are synthetic long chain polymers produced by continuous polymerization/spinning or melt spinning. The most common usage in radial passenger tires is as cap, or overlay ply, or belt edge cap strip material, with some limited applications as body plies. Advantages: Good heat resistance and strength; less sensitive to moisture. Disadvantages: Heat set occurs during cooling (flatspotting); long term service growth.

<u>Polyester</u>: tire cords are also synthetic, long chain polymers produced by continuous polymerization/spinning or melt spinning. The most common usage is in radial body plies with some limited applications as belt plies. Advantages: High strength with low shrinkage and low service growth; low heat set; low cost. Disadvantages: Not as heat resistant as nylon or rayon.

Rayon: a body ply cord or belt reinforcement made from cellulose produced by wet spinning. It is often used in Europe and in some run-flat tires as body ply material. Advantages: Stable dimensions; heat resistant; good handling characteristics. Disadvantages: Expensive; more sensitive to moisture; environmental manufacturing issues.

Aramid: a synthetic, high tenacity organic fiber produced by solvent spinning. It is 2 to 3 times stronger than polyester and nylon. It can be used for belt or stabilizer ply material as a light weight alternative to steel cord. Advantages: Very high strength and stiffness; heat resistant. Disadvantages: Cost; processing constraints (difficult to cut).

Steel cord: carbon steel wire coated with brass that has been drawn, plated, twisted and wound into multiple-filament bundles. It is the principal belt ply material used in radial passenger tires. Advantages: High belt strength and belt stiffness improves wear and handling. Disadvantages: Requires special processing, and it is more sensitive to moisture.

Bead wire: carbon steel wire coated with bronze that has been produced by drawing and plating. Filaments are wound into two hoops, one on each side of the tire, in various configurations that serve to anchor the inflated tire to the rim.

2.4.1 Textile Reinforcement

There are at present, five main types of organic fibers used in reinforcement for rubbers [4]. They are, cotton, rayon, polyamides (previously referred to as nylon), polyester and aramids. It is worth mentioning that in Europe, the term synthetic is used only when referring to fibers in which the fiber-forming polymer is not of natural origin [4].

As most of these reinforcement materials were already mentioned, only cotton is in need of a brief introduction, as follows [5]:

Cotton: it is a 100% natural cellulose fiber. It absorbs humidity form air (approximately 8%) and swells in water, but the wet strength of the yarn can improve up to 20% from that in the dry state. When drying, the properties revert to the original. It has generally good resistance to heat up to 150°C, but on prolonged exposure between 100°C and 150° and above 150°, it will lose strength. Its decomposition starts at around 230°C. Cotton burns readily, but in low oxygen concentration it will char and leave a carbon skeleton.

2.4.2 Steel Reinforcement

2.4.2.1 Steel Cord

Steel is a metal alloy whose major component is iron, with carbon content between 0.02% and 1.7% in weight. Carbon is the most cost effective alloying material for iron, but many other elements are also used. Carbon and other elements act as hardening agent, preventing dislocations in the iron atom crystal lattice from sliding past one another. Varying the amount of alloying elements and their distribution in the steel, controls qualities such as hardness, elasticity, ductility and tensile strength of the resulting steel. Currently, there are several classes of steels in which carbon is replaced with other alloying materials, and carbon, if present, is undesired [6].

Steel cord is a major component used for reinforcing a radial tire. Steel cord is stronger than fibre materials, have excellent heat resistance, fatigue resistance, with no contraction. Steel cord is a tire reinforcement material with the highest growth rate [6].

2.4.2.2 Steel Cord Components

A steel cord is composed by four components, as shown in *Figure 6*. A description is presented below [7]:

Filament (1) – Individual element of a Strand and Cord.

Strand (2) – Group of Filaments combined together.

Cord (3):

- ✓ End product of 2 or more Filaments.
- ✓ End product of 2 or more Strands.
- ✓ End product of a combination of Filaments and Strands.

Wrap (4) – Filament wound helically around the Cord.

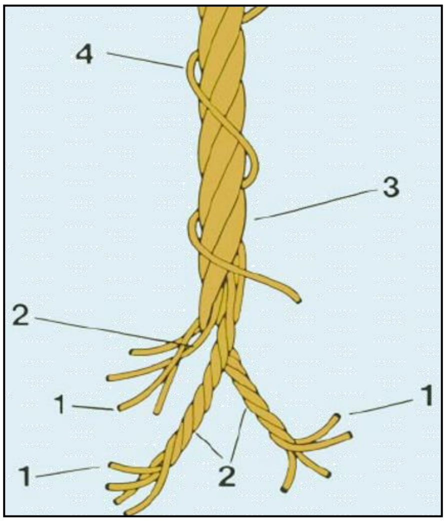

Figure 6- Steel Cord Components [7]

2.4.2.3 Steel Cord: General Characteristics

A steel cord is composed by wire rod as a raw material. The tensile strength values of each are related to the content of the ingredients. *Table 1* summarizes the main aspects.

Table 1 – Average steel composition of steel cords [7]

Composition	Normal Tensile	High Tensile	Super High Tensile
Carbon	0.7	0.8	0.9
Manganese	0.5	0.5	0.5
Silicon	0.2	0.2	0.2
Sulphur, Phosphorus	0.015	0.013	0.013
Copper, Chromium, Nickel	0.05	0.05	0.05

2.4.2.4 Steel Cord Design

When focusing on the design of steel cords, there are two possible orientations, regarding the lay direction, being these presented as follows, and also, possible to be seen on *Figure 7* [7]:

Lay Direction: Helical arrangement of Strand/Cord:

- Z direction (right hand lay): Spirals conform the central portion of Z.
- S direction (left hand lay): Spirals conform the central portion of S.

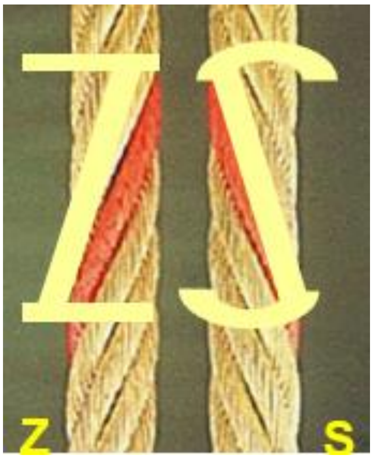

Figure 7 – Arrangement of Strand/Cords [7]

2.4.2.5 Steel Cord Types

There are many types of cords depending on the purpose of its applications and the intended twist level. The most common cord types are presented as follows and in *Figure 8* [7]:

1. Regular Cord: Direction of Strands in opposite to direction of Cord.
2. Lang's Lay Cord: Direction of Strands and Cord is the same.
3. Open Cord: Filaments are loosely associated to enable a high compound penetration.

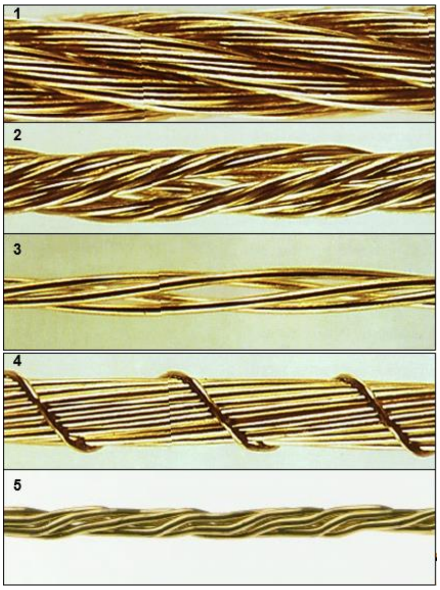

Figure 8 – Steel Cord Types [7]

4. Compact Cord: Cord Filaments are tightly packed.
5. High Elongation Cord: Preformed Filaments of short lay length (3mm) for ensuring high structural elongation.

2.5 Adhesion between Steel Cord and Rubber

Steel cord has been the main reinforcing material for tires, hoses, and conveyor belts for many decades, indeed the first steel reinforced tires appeared over ninety years ago. However, it was not until the emergence of radial tires that steel cord became a common form of reinforcement and understandably the adhesion between brass-coated steel cord and rubber compound became a significant factor governing the performance and durability of car and truck tires. Therefore, it is necessary to achieve a high level of adhesion and sustain this level throughout the service history of the tire [8].

However, the rubber-metal interface is prone to deterioration, particularly under dynamic conditions of high humidity and salt, and so reinforcement by the steel cord is reduced, with a concomitant reduction in the life of the tire. Consequently, various organic cobalt salts are used, alone or in combination with resin systems, to improve and maintain good bonding at the rubber-metal interface. At present, organic cobalt salts appear to be the most efficient adhesion promoter and could be considered as a bench-mark by which the tire industry assesses rubber-metal bond strength [8].

2.5.1 Mechanisms of rubber-brass bonding

When forming a tire cord, copper and zinc are electro-deposited sequentially on to drawn steel wire and treated by a thermal diffusion process to produce a brass alloy coating. Further drawing of the wire eventually produces a steel cord filament coated with a brass layer, approximately 0.2 μm thick. When the metal filaments are drawn, it is possible that organic residues from the lubricant baths are deposited on the brass surface and these may affect the adhesion of the rubber to metal after vulcanization. Typically, a brass layer is composed of 63.5% cooper and it has been shown that the adhesion force tends to a maximum value with a cooper content between 67% and 72%, but better retention of adhesion after ageing under humid conditions is achieved at a lower copper content. Adhesion can also be affected by differences in the concentration of zinc and copper in the surface compared to the composition of the bulk brass. If the brass coating is insufficient then corrosion resistance is lowered and poor adhesion can occur after ageing. This is due to delamination of the brass by dissolution of iron in exposed areas that can eventually result in cord breakage [9].

When brass-coated wire is drawn during the formation process, Zn^{2+} ions diffuse to the surface and oxidized to form a ZnO layer. A thin CuO skin can form, but it is usually present in very small amounts. The enriched ZnO layer also contains metallic cooper inclusions formed as a result of the internal oxidation mechanism of zinc [9].

During vulcanization, exposure of the brass surface to active sulphur containing molecules creates a strong bond by the action of an interfacial, non-stoichiometric copper sulfide layer that grows before the rubber is fully crosslinked. At an early stage of vulcanization, copper ions, zinc ions and free electrons move to the surface of the brass wire via cationic diffusion and a copper sulfide layer, with some zinc sulfide, is formed via a process called sulfidation. As cooper sulfide and zinc sulfide tend not to form mutual solid solutions there will be a tendency to phase segregate. Zinc sulfide forms initially, but at a later stage it is overgrown by cooper sulfide and the rate at which the critical thickness of cooper sulfide is reached has been attributed to the much faster rate of formation of copper sulfide to that of zinc sulfide [9].

The rate of copper sulfide formation is sufficient to allow growth to a thickness that is essential for a good bond formation and the amount of cooper sulfide formed depends primarily on the number of copper inclusions in the initial zinc layer. It has been stated (van Ooij) that sulfidation will cease when all the copper inclusions are depleted but other studies revealed that the presence of accelerator moieties was a significant factor. The amount of cooper sulfide present in the layer is directly related to the degree of sulfidation and it is essential to delay the cross-linking process long enough to build a copper sulfide layer of critical thickness [9]. *Figure 9* allows to have the perception on the change brass-rubber interface, before and after vulcanization.

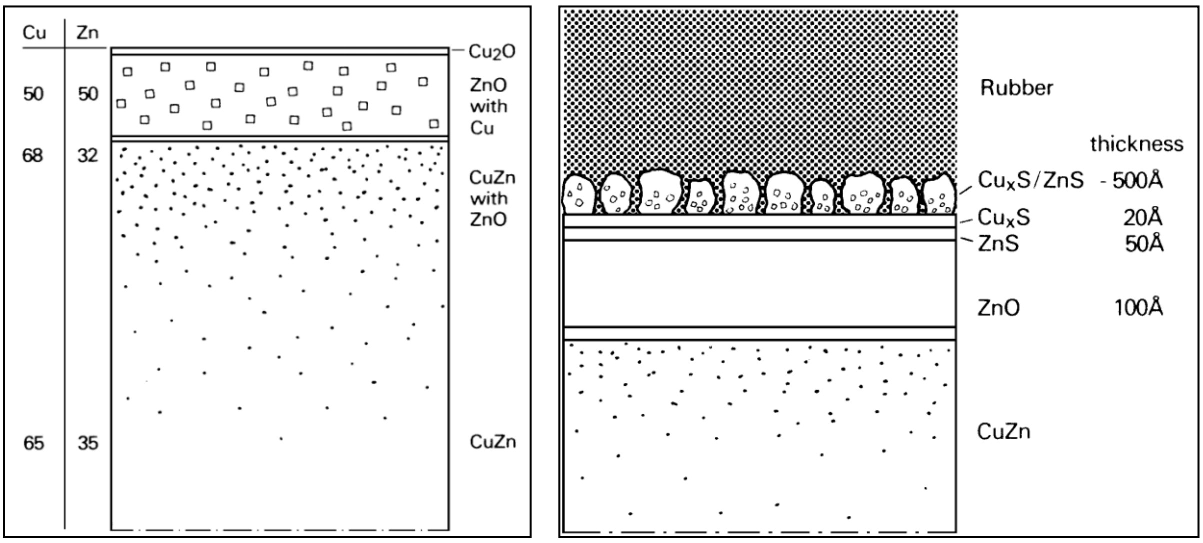

Figure 9 – Typical brass-rubber interface before (left) and after (right) vulcanization (Adapted from [9])

2.6 Ageing of the rubber-brass interface

Rubber-brass bond degradation may be due to several processes, including thermal ageing and electrochemical corrosion. During heat ageing, degradation of the rubber as well as deterioration of the interface may occur. Copper migrates, by cationic diffusion, through the zinc sulfide and copper sulfide to thicken the existing copper sulfide layer and weaken the rubber-metal bond [9].

When the copper sulfide layer stops growing, zinc ions diffuse through the entire interfacial layer to create more zinc oxide. The diffusion of zinc ions can be a slow process under dry conditions; but, eventually, zinc oxide will develop at the metal surface to weaken the bond. In humid conditions, an increase of moisture and oxygen content will accelerate this process by altering the rate of diffusion of the zinc ions [9].

In due course, the formation of zinc oxide from the precipitation of zinc destroys the integrity of the copper sulfide layer and debonding occurs. Such processes are generally called dezincification and are assumed to be the major, underlying effects that cause bond failure [9]. In *Figure 10* it is possible to verify the mechanism of dezincification.

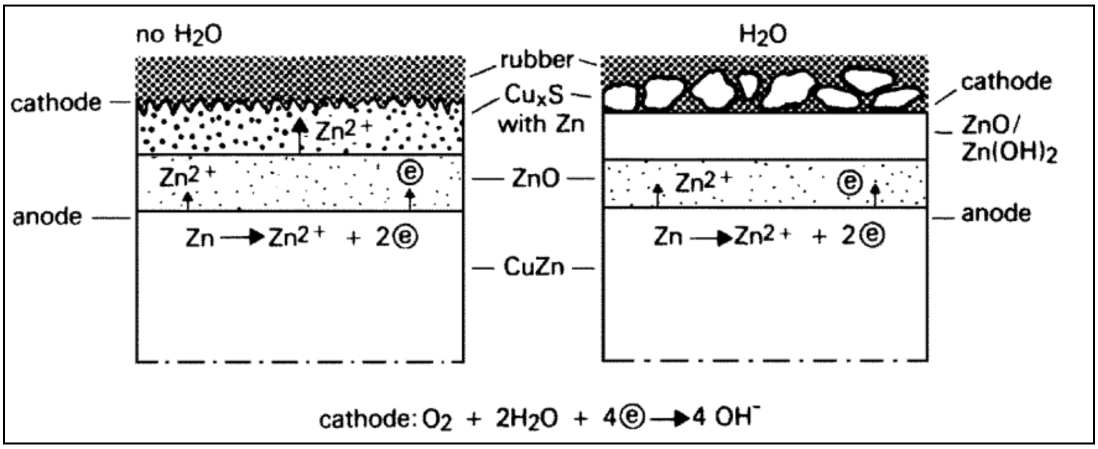

Figure 10 – Interfacial structures formed after ageing of the rubber-metal bond [9]

2.7 Static and Dynamic Tests

A large number of tests have been developed to help in the evaluation of adhesion force and are basically either static or dynamic in nature. In the tire industry, most of the methods used for determining adhesion force are static in nature [10]. The static and quasi-static tests, such as the H-pull (H-adhesion) test, peel and wedge-cleavage test, are not suitable to predict the durability if the system in the real conditions [11].

Although these methods are helpful in detecting obvious deficiencies of cord rubber bonding, they are not sensitive to subtle changes and do not take into account influencing parameters that have negative effect on the interfacial adhesion, such as the temperature, humidity, oxygen, and ozone. Moreover, the nature of the tests is not simulating the service conditions of the tire. As a result, the data obtained are not an indication of the real performance of the product. Therefore, the dynamic tests are of great importance and meaningful as far as prediction of durability of the tire is concerned [10].

Most of the dynamic test methods can be classified into four major categories on the basis of the mode of deformation e.g., tension, compression, shear and flexing. Popular dynamic test techniques are [10]:

- The Buist dynamic Test
- The Iyenger Method
- The Voracheck Method
- The Khromove method
- The Wagner disc-fatigue method

2.7.1 Tension Test Methods

There are two types of tension test methods. In the first, either the rubber is fixed and the cord or the metal plate is tensioned directly or else this situation is reversed. In either case, the cord is difficult to deform and the rubber moves easily and so a repeated shear strain is applied to the cord-rubber boundary surface, and the test causes fatigue deterioration of the adhesion to occur. The second method is the repeated tension peel method [12].

2.7.1.1 Tension Method

The tension method is the most typical method of evaluation of all the dynamic adhesion fatigue tests and it is the most frequently used method since it has the advantages that a partly modified De Mattia Tester (*Figure 11)* or a conventional rubber tension fatigue tester can be used and the evaluation is easily made [12].

Figure 11 – De Mattia Tester

2.7.1.2 Peeling type test method

Concerning the peeling type test methods, the reasons for the scarcity of reports on the subject of dynamic test methods are the difficulties experienced in maintaining a constant peel surface and peel angle during a test and the difficulties that are experienced in connection with the accuracy of the peel force. However, it is thought that with peel type adhesion fatigue test methods a comparison of static evaluations and dynamic evaluations is easy, the test machines themselves are comparatively simple, and therefore there is a cost advantage [12].

2.7.2 Compression Test Methods

There are two types of compressive adhesion fatigue test. The first type was introduced in part in connection with the tensile type adhesion fatigue test methods, being a falling weight repetitive impact type test. The other type involves the use of a flexometer in which a compressive deformation of fixed amplitude is applied under a fixed compressive load [13].

2.7.2.1 Impact type test methods

The Dunlop Fatigue Tester, a punch type tester machine, was first described in 1941. With this machine, the repetition rate onto the rubber block which forms the sample is 150-300 times per minute. With this tester, parameters such as fixed load, fixed displacement and fixed energy tests can be carried out. As a result, and alongside with constant improvements implemented over the years, the majority of the test methods available have evolved from this tester.

2.7.2.2 Flexo-type test methods

This kind of test methods involves embedding a cord in a sample and assessing the adhesion fatigue degradation after repeated compression using the flexometer. The distinguishing features of the “flexo” system are that the adhesion fatigue degradation is produced at the cord-rubber bonding surface by a shear strain that results from the compression, simulating the situation in a running tire [13].

3. Test Development Description and Discussion

In this chapter, the focus is to go over the test methods that were developed during this internship. Explanations of the procedures are performed, as well as the necessary implemented changes, alongside with the references to the involved machinery.

3.1 3 Cord Adhesion Test

This test method, both static and dynamic, allows for the study of the adhesion between rubber and steel cords. The main purpose is to measure the force required to peel steel cords from the rubber matrix, after each of the three different stages of the test method: fresh sample, aging condition and fatigue deterioration.

The dynamic part of the test, occurs when the sample is submitted to fatigue deterioration, which is very important, in order to extend the understanding of the variables interfering with the sample, as well as through the simulation of the conditions imposed, when comparing it with a rolling tire.

Fresh Sample

After vulcanization occurs, it is necessary to wait for a certain period of time in order to start the first stage. The objective is to place the sample at the Zwick Tensile Tester Machine, available at the laboratory, and peel the cord sets from the rubber sample, at room temperature, as visible on *Figure 12*. The number of steel cords on each cord set may vary, although it is usually composed by 3 steel cords.

At this stage, it is expected that the peel force is the highest.

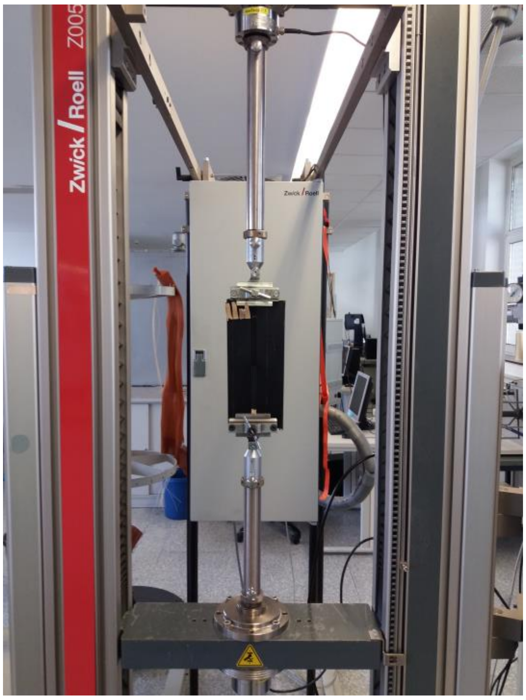

Figure 12 – 3 Cord Adhesion Test – Peeling of the steel cords

Aging Condition

The second step consists in placing the sample inside a high pressure container with water, *Figure 13*, to submit it to an aging process which can last for a period of 2 days to a period of 15 days, depending on the experiment. The oven where aging occurs, *Figure 13*, can operate under a steam condition, being the temperature 105°C, or under a humidity condition being the temperature 70°C.

Before introducing the sample inside the container, it is mandatory to apply a specific anti-corrosive primer based on pure PVC-resin (REESA PVC-Primer 3G050), *Figure 13*, on top of the existing gaps created for the previous peeling test. This is due to the fact that these gaps would create an area where the aging condition would be more intense, making it non-uniform.

Figure 13 – Oven (left), high pressure container (centre) and anti-corrosive primer (right)

Fatigue Deterioration

The last stage of the test method is the fatigue deterioration. This is where the dynamic testing takes place. It may be conducted either on the Frank Machine or on the MTS Machine. Since the MTS machine has shown better results in the past, due to the fact that it allows the operator to choose the working temperature, it should be the selected device to carry on with the test.

On this machine, the executed dynamic test allows the sample to be constantly bent until reaching a fixed number of cycles, frequency and temperature, under a relatively short amount of time. This bending is of extreme importance, taking into account that it represents the closest behavior to the one happening on a real tire service condition.

Regarding the parameters involved, either the amplitude or the force are fixed. While performing fatigue deterioration on the MTS Machine, a measurement of the force is mandatory to guarantee that the behavior evolves as expected. In other words, a measurement of the force reveals a decrease with time, resulting from the fact the sample's properties are under stress and, as a consequence, its integrity decreases.

3.1.1 3 Cord Adhesion Test – Internship Starting Scenario

The initial goal of this internship, regarding this test method, would be to assess the behavior of new materials in order to realize which kind of compounds would behave similarly to the ones used on a regular basis.

According to previous work developed at Continental, the test method was already established, meaning that all the steps from the sample building process to the testing set-up, have already been set.

However, it was possible to acknowledge in preliminary studies, while learning how to build the samples and how to conduct the tests, that it was necessary to review all the steps regarding the test method itself, from the very beginning, due to regular inconsistencies detected on the fresh sample phase, after several measurements of the peel force.

Hence, the execution of the two remaining phases was not performed, and new compounds were not able to have been tested.

Table 2 summarizes all the studies performed throughout the internship. Due to the fact that it was necessary to implement changes regarding the configuration of the samples, two configurations were defined. From the moment the internship started, the configuration is named as "Starting Configuration", and after implementing the necessary changes is presented as "Upgraded Configuration".

Table 2 – Tests performed for the 3 Cord Adhesion Test

Topic/effect under study	Starting Configuration	Chapter	Upgraded Configuration	Chapter	Decision
Symmetry and Orientation	✓	4.1.1	✓	-	Keep symmetry and orientation
Number of cords per cord set	✓	4.1.2	✓	4.1.7	3 Cords per Cord Set
Waiting time	✓	4.1.3	✓	4.1.8	48-72 hours
Visual Inspection	✓	4.1.4	✓	-	Analyzed on every sample
Back Layer Angle vs waiting time	✓	4.1.5	X	X	22° and 48 hours

3.1.2 3 Cord Adhesion Test – Sample Building and Testing Procedures

The rubber compound used on every sample is referred to as “standard”. The provided rubber material had on the inside calendered steel cords. To start, it was necessary to cut two layers of it, the dimensions of each being: 26 cm length, 9.5 cm width and 1 cm thickness. The front layer, the one where the steel cords are to be peeled from, has an angle of 0°, while the back layer has an angle of 22°. Both are placed on top of each other and inserted in the molds available at the laboratory. Due to the fact that there were no specified reasons for the back layer angle, studies were conducted in order to check the relevance of this parameter on the results.

The heat press machine where vulcanization takes place, must be pre-heated to the working temperature of 150°C. The pressure is 57 bar, and the process last for 30 minutes.

After vulcanization, it is necessary to leave the samples to cool down for a period of time, starting from 3 hours.

Only after this period, the testing procedure can start. Since there was no real conclusion of the importance of this waiting period and its effects on the results, studies were conducted and are presented on Chapter 4.

At the Zwick Tensile Tester machine, it is important to choose clamps which minimize friction during the test. Friction can have a huge impact on the results obtained by the software and it can lead to invalid test results on extreme cases.

It is imperative to zero the clamps every time a cord set is peeled out. It is also essential to place the sample in a configuration that will allow the cord sets that are meant to be peeled, to be in the center of the clamps, *Figure 14*. Furthermore, if the peeling occurs for a cord set containing 2 or 3 steel cords, it’s advisable to use duct tape to ensure that all the cords will be pulled at the same level at the same time, otherwise the results might differentiate, *Figure 14*. After finishing each specimen, the steel cords must be removed from the sample so that friction is minimized for the upcoming specimens.

Figure 14 – 3 Cord Adhesion Test Starting Configuration

Regarding the testing parameters, the test speed should be 50 mm/min and the length of the test 250 mm, although, as default, the first 10 mm and the last 10 mm are not taken into evaluation.

3.1.3 3 Cord Adhesion Test: Notation and Original Sample Configuration

In order to understand the results presented on the next chapter, it is necessary to clarify some of the notation implemented on the samples.

The starting structure of each sample is composed of 10 cords sets. Usually, each cord set contains 3 steel cords. Depending on the width of the sample, there were cases when only 9 cords sets were able to peel.

Throughout testing it is important to maintain the symmetry of the sample, which means that every time a cord set is peeled out, from the ends to the center of the sample, a rotation of it is required. The letter “N” refers to normal orientation of the sample, and “UD” refers to upside down. The orientation of the sample is defined from the moment when the building process starts, marked with an arrow.

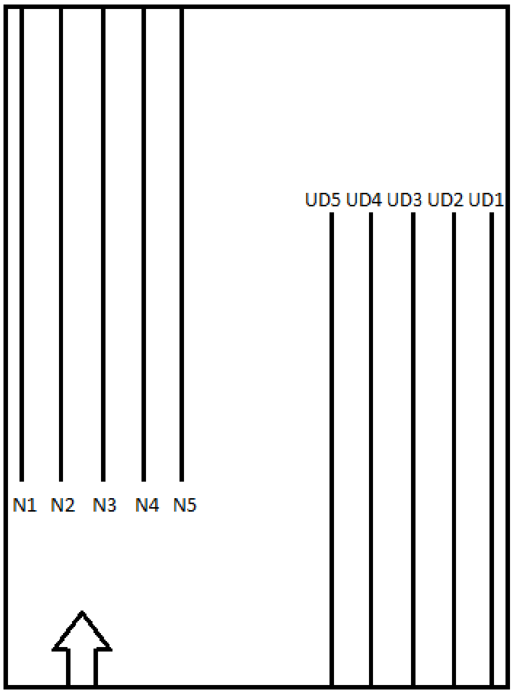

Figure 15 – Adopted Notation

3.1.3.1 3 Cord Adhesion Test: Upgrade on the sample configuration

Due to the fact of constant irregular results, which ended up affecting the reproducibility of the test method, a change in the configuration of the sample was necessary to implement.

According to the data obtained, it became clear that the force required to peel out the cord sets usually increased towards the center of the sample (this results will be detailed on the next chapter).

Many reasons could be causing this behavior, and in order to avoid it, it was necessary to exclude the peeling of the cords sets in this central area. Hence, the number of cord sets was reduced from 10 to 6 cord sets, meaning 2 cords sets per stage (fresh, aging and fatigue).

Another upgrade necessary to implement, was related to the fact that the cutting device available at the laboratory was not able to provide the best surfaces on the samples, and this could have a huge impact when placing them inside the mold, to proceed to vulcanization.

A premise, regarding the sample building process, states that there can be no gaps when placing the sample inside it. Since this premise was very hard to guarantee, to make sure that these irregularities could be minimized, the size of the sample was diminished by a centimeter both on length and width, being this difference filled with regular rubber without calendered cords, *Figure 16*. *Figure 17* shows the difference between the samples.

Figure 16 – Upgraded Sample Configuration (non-vulcanized sample)

Figure 17 – Starting Configuration) (left) and Upgraded Configuration (right)

3.1.4 3 Cord Adhesion Test: Equipment

3.1.4.1 Zwick Tensile Tester

Commercially known as AllroundLine, this machine is suitable for applications in all fields. It is ideal for quality-control testing or as a part of research projects. It is available with test speeds from 0.00005 to 3000 mm/min. The testing machine speed is independent of test load, and is available for test loads up to 250 kN and test-area heights from 1030 mm to 2560mm. It can be operated with standard commercial PCs or laptops [14]. On *Figure 18*, it is possible to observe the apparatus.

3.1.4.2 MTS Machine

The MTS machine is the device used to perform the test fatigue procedure, *Figure 18*. Specifically, the model is MTS810 and its features include a force range from 25kN to 500 kN, the ability to test materials ranging in strength from plastics to aluminum, composites and steel; a large test space to accommodate standard, medium and large specimens, grips and environmental subsystem; the capability to perform a wide variety of test types from tensile to high cycle fatigue, fracture mechanics, and durability of components [15].

Figure 18- Zwick Tensile Tester [14] (left) and MTS Machine [15] (right)

3.2 Oldy Test

The second test method under study on this master thesis is the Oldy Test. It is a very recent test method developed by Continental and it allows the assessment of the adhesion of textile cords to the rubber samples, with different adhesion promoters (AP). It is performed on the machine present on *Figure 19*, and it provides the possibility to perform both a static test and a dynamic test. The frequency imposed is 5 Hz, the displacement is ± 25 mm and the control mode of the machine is possible by displacement.

The dynamic test is conducted with the purpose to evaluate the amount of cycles a sample can last for, depending on the chosen compounds for the rubber and the textile cords.

According to the mold available at the laboratory, 8 samples are built for each compound, at the same time. Regarding the dimensions and the type of sample used on this test method, a non-vulcanized sample is present on *Figure 20*.

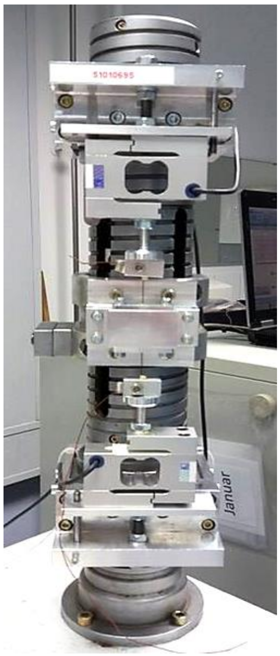

Figure 19 – Oldy Test Machine

Although the sample is very simple, the sample building process is quite extensive, and it is present in the Appendix 1.

Regarding the vulcanization process, it is conducted at 170° for 10 minutes.

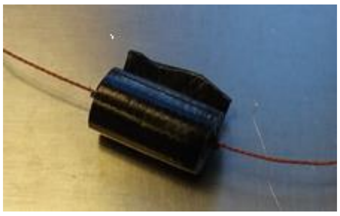

Figure 20 – Oldy Test Sample (non-vulcanized)

3.2.1 Oldy Test Testing Procedure

The testing procedure is divided in two parts, as shown on *Figure 21*. In the first one, the static part is conducted and it should last for a period of 600 seconds. The goal is to submit the textile cord, which is attached to the extremes of the machine, as shown on *Figure 22*, to an input tension, until reaching a constant level of force, which varies according to the type of compound under study, as well as its breaking force.

In the beginning of the static test, due to the fact that the cords are submitted to a very high amount of force in a matter of seconds, the relaxation time for the cords to adapt to it is much shorter, when comparing to the amount of time during the last part of the static test. During this part, the computer is monitoring the force throughout time.

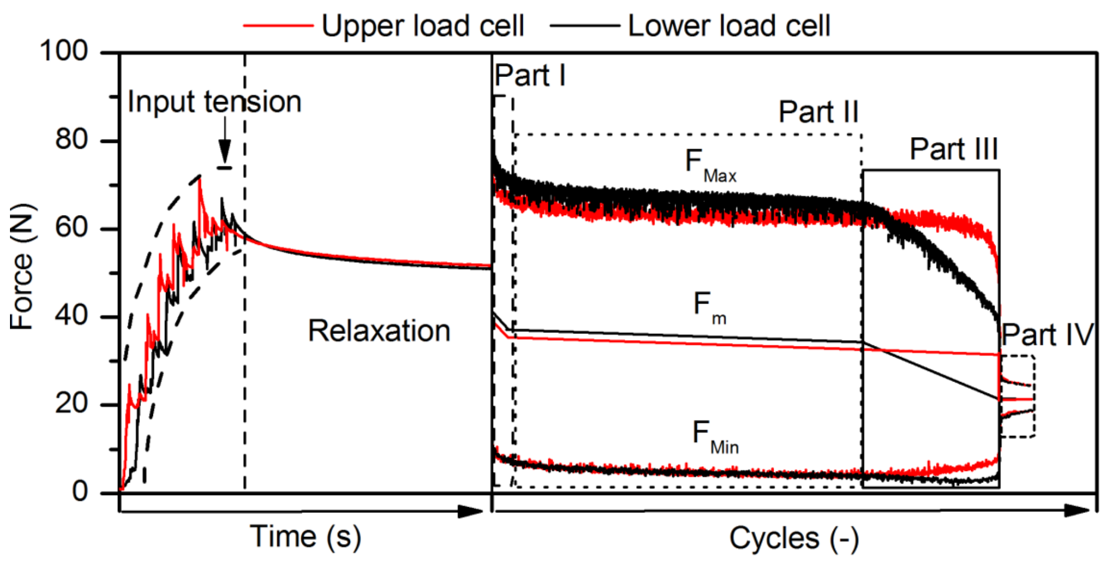

Figure 21 – Computer output of a standard measurement [16]

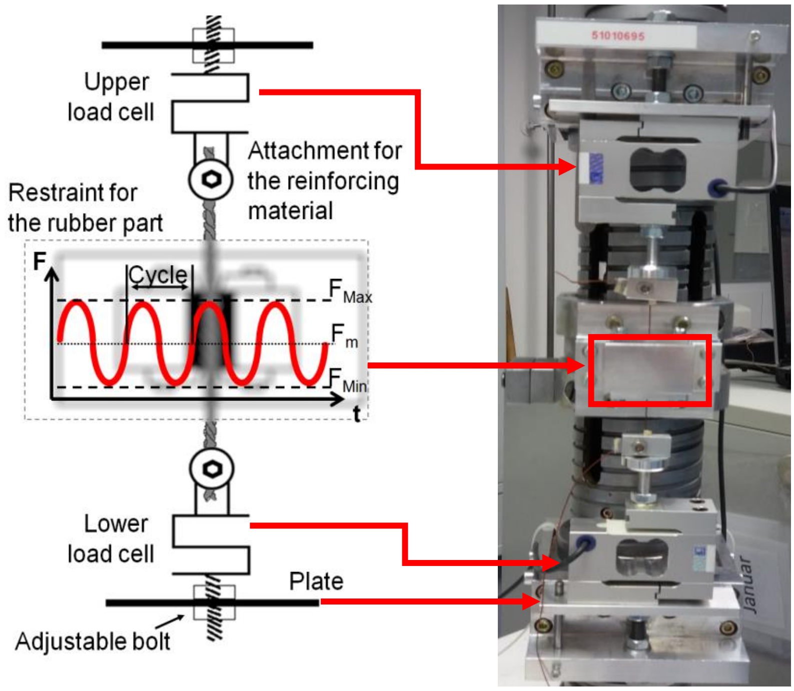

Figure 22 – Schematics of the apparatus (left) (Adapted from [16]) and Oldy Test Machine (right)

The second part of the test, is the dynamic one. The goal is to motorize the force throughout the number of cycles. The dynamic part is divided into [16]:

- Part I: Adaptation

- Part II: Compensation-Induction
- Part III: Adhesion looseness
- Part IV: Residual resistance

The machine is under a fixed cyclic displacement, according to a chosen amplitude, until the rubber sample detaches from the textile cord.

Depending on the adhesion promoter (AP) under study, the number of cycles will vary, as well as the force required to conduct the test. An illustration of this behaviour is present of *Figure 23*.

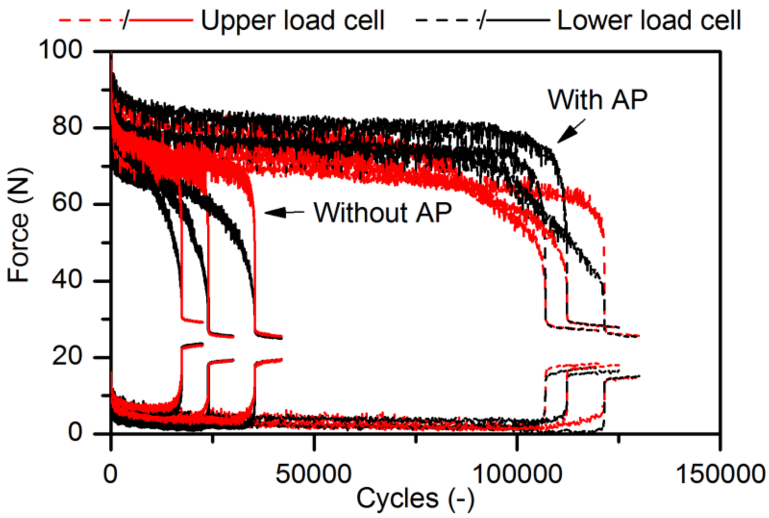

Figure 23 – Dynamic part of the Oldy Test. Illustration of the influence of Adhesion Promoters [17]

4 Results and Discussion

4.1 3 Cord Adhesion Test

4.1.1 The effect of Orientation and Symmetry

While performing the first tests on the Zwick Tensile Tester, many types of charts with different behavior were obtained.

At this early stage of the internship, it was expected that the force throughout the test for the 250 mm under evaluation would show a constant pattern, at least for the majority of the extent under evaluation as shown in *Figure 24*. Hence, the orientation of the sample was not supposed to have an influence on the results, due to the fact that both the front and back layers of the samples would continue to have the same orientation, 0° and 22°, respectively.

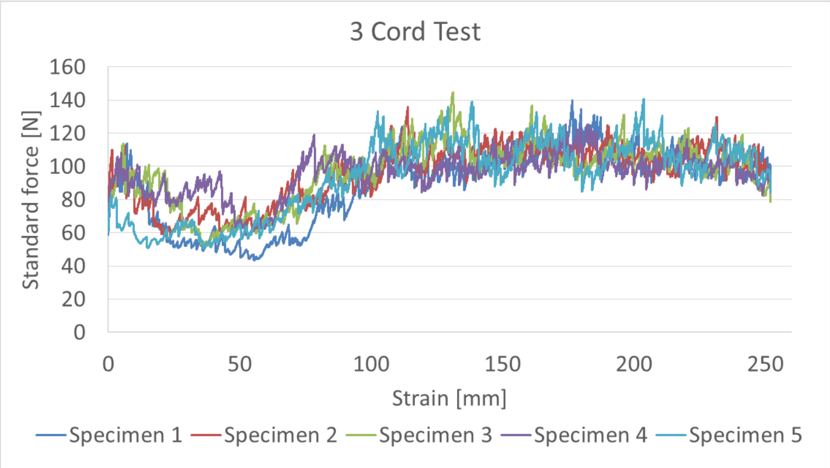

Figure 24 – Expected behaviour for the 3 Cord Adhesion Test

However, it was easily noticeable that, from sample to sample, the force varied too much. As a consequence, it became mandatory the need to set an orientation, starting at the sample building process, to be able to compare the results.

Furthermore, the peeling of the cord sets should also be done symmetrically and not only from one extreme of the sample to the other, as it was the case before. In other words, to keep the integrity of the samples constant throughout the test, the peeling of cord sets was done by the following order of cord sets: N1 followed by UD1, N2 followed by UD2, and so on.

As a conclusion, all the results from Chapter 4.1.3, will take these two factors in consideration.

4.1.2 Impact of the number of Cords on each Cord Set

The next step regarding this test method, was to assess if the number of cords per each cord set being peeled from the samples, would have a relevant influence on the behaviour of the force.

After analysing the charts presented on *Figures 25-27*, it is clear to verify, at first, that 1 cord test would be the best choice to continue with the test method, due to a constant level of force throughout the majority of extent under evaluation.

However, taking into account Figures 26 and 27, since the force varies too much and is not constant, the need to specify an interval in which the force varies the minimum, was necessary to implement, so that all scenarios could be compared.

Hence, while performing the tests on Sample 5, and after considering these intervals, it became clear that, according to the deviation obtained by the software connected to the Zwick Machine, the best suited number of cords per each cord set, would be 3. On *Table 3*, it is summarized the information regarding the number of cords, the interval chosen for evaluation, as well as the deviation obtained.

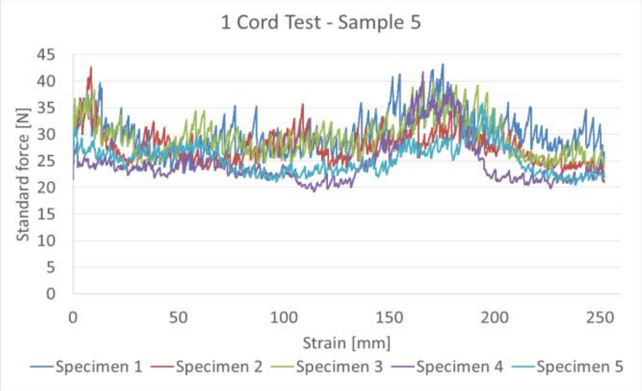

Figure 25 - Evolution of the force for 1 cord per cord set

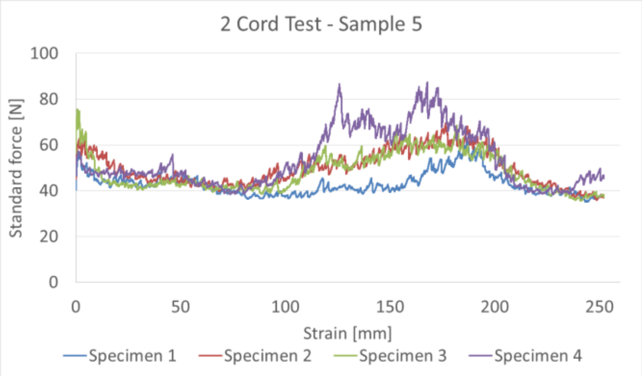

Figure 26 - Evolution of the force for 2 cords per cord set

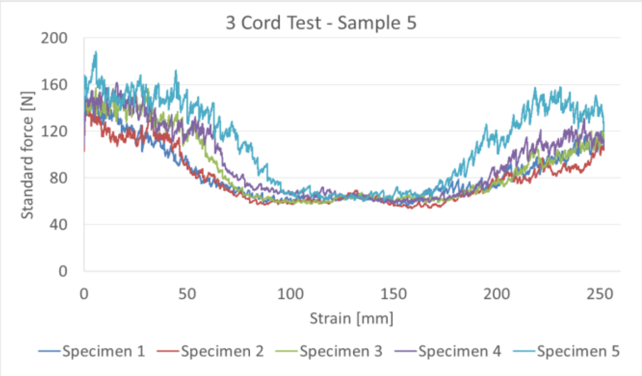

Figure 27 - Evolution of the force for 3 cords per cord set

Table 3 – Resumed data of the impact of the number of cords per cord set

Number of cords	***Interval of evaluation (mm)***	***Deviation***
1	50-150	3.1
2	20-110	3.0
3	90-170	2.3

4.1.3 The waiting time effect

In order to understand the impact of the waiting time on the results before performing the test, and since this type of study was never performed before, 4 samples were built and tested at different times.

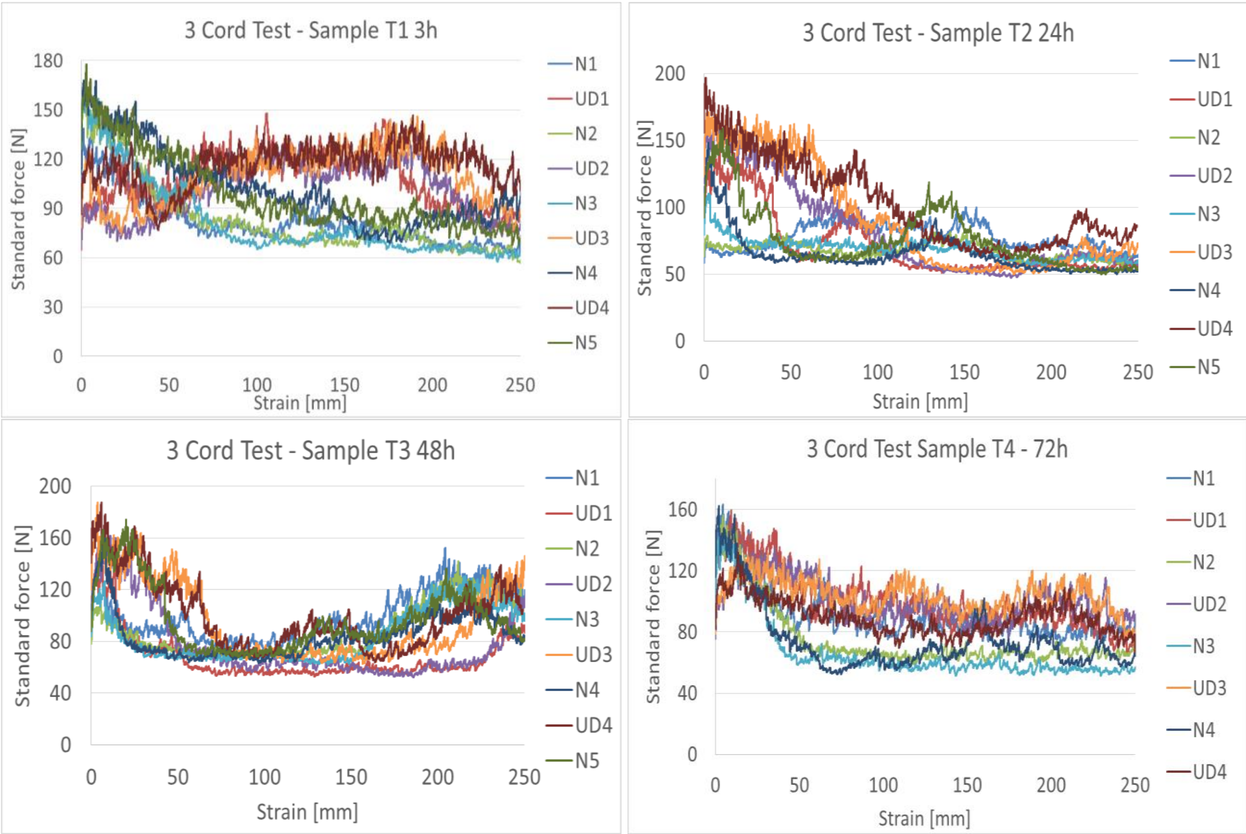

Figure 28 – Illustrations of the 3 Cord Adhesion Test for different waiting times

Figure 28 summarizes the 4 scenarios. Going over each one, it is easy to realize that after 3 hours, the evidence of extreme behavior is noticeable due to the presence of two distinct levels of force. For Sample T1, the cord sets with a normal orientation require a minimum force to be peeled out, while those with an upside down orientation require a force which is around the double of the magnitude.

After waiting 24 hours, the pattern obtained reveals some improvement, and despite the fact that the initial 50 mm of measurement reveals again two levels of force, during the last 150 mm, the force tends to stabilize in one level only.

For 48 hours an unexpected behavior was obtained, because throughout the sample and after the first 50 mm of measurement (during which the samples are more susceptible to friction with the clamps) the force increases.

Finally, and for the longest waiting period, although Sample T4 reveals a range of force that varies in magnitude around 60 N, it is the one where the pattern is the same regardless of the orientation of the cord sets.

After this study, although the results show a discrepancy related to the test method configuration set-up, the most suitable choice would be to wait for the execution of the 3 Cord Adhesion Test for a period between 48 hours of 72 hours.

4.1.4 Visual Inspection

Since, usually, every sample shows two different levels of force, it was necessary to take a closer look at the surface of the samples after the tests, and try to perceive if a regular pattern is present. After the execution of this exercise, it was possible to notice that the cord sets with the orientation that needed the highest amount of force to be peeled, were the ones leaving a more wrinkled pattern on the samples. An example of one of the most extreme behaviors is present on *Figure 29*.

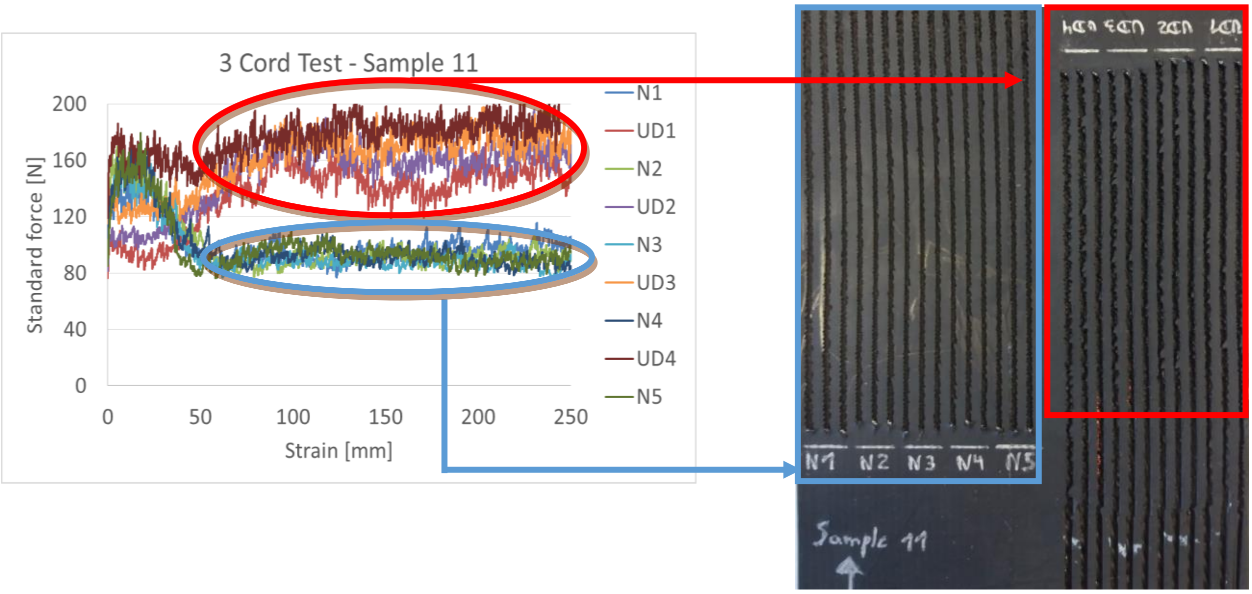

Figure 29 – Evolution of the peel force throughout the sample (left) and visual inspection of the samples surface (right)

Even though, in the presented sample, the more wrinkled pattern was obtained for the cord sets with the upside down orientation, this was not always the case, making it more difficult to realize what may be causing this problem.

4.1.5 Back layer orientation vs. waiting time effect

Another parameter which has never been studied before was related to the angle of the back layer. According to the available sample building procedure, and after considering all the information obtained, there was not a specific reason for the angle of 22°.

Considering that, until this point, the obtained results were revealing an inconsistent behavior, a change in the angle of the back layer was performed, alongside with the study of the time effect, once again, in order to verify if it would be possible to obtain a pattern. Hence, 4 back layer angles were studied: 0°, 22°, 45° and 90° for periods of 48 hours and 72 hours.

Furthermore, to better understand the evolution of the peel force from the cord sets placed at the extremes of the sample, to those placed on the center of it, charts as the one presented in *Figure 31* were elaborated. On the X-axis, it is focused the cord sets being compared "N1-UD1", "N2-UD2", "N3-UD3", and "N4-UD4", and on the Y-axis it is shown the absolute value of the difference of the force. The data from which the charts on *Figures 31, 33, 35,* and *37* were created, are present on the Appendix 2.1.

4.1.5.1 Back layer angle of 0° for 48 hours and 72 hours

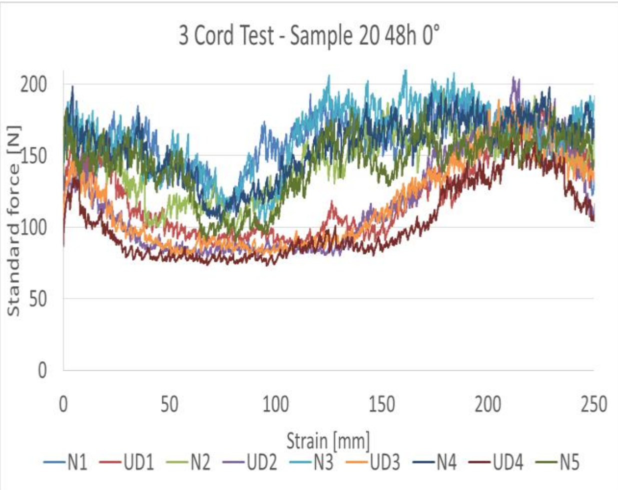

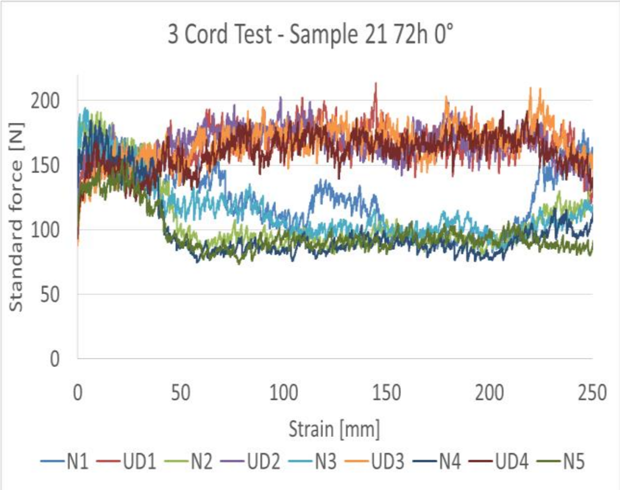

Figure 30 – Evolution of the force for a back layer of 0°

As it can be acknowledged from the charts presented of *Figure 30*, the extreme behaviour is present again. With a back layer angle of 0°, moving towards the central cord sets, the force tends to increase, *Figure 31*, and the waiting time effect provides a low influence on the magnitude of the force. Regarding the stiffness of the sample, it is very high, and in practical effects, it is far from ideal.

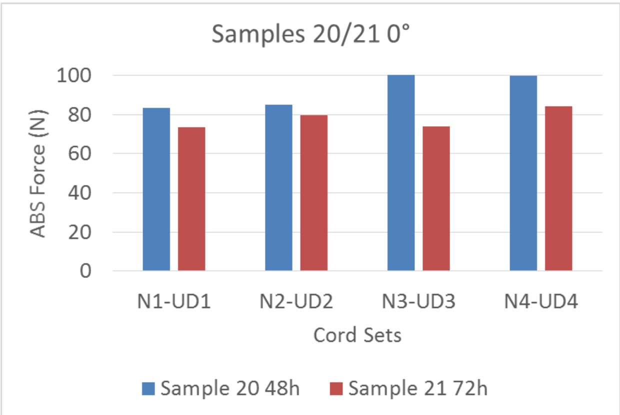

Figure 31 – Evolution of the force towards the centre of the samples 20 and 21

4.1.5.2 Back layer angle of 22° for 48 hours and 72 hours

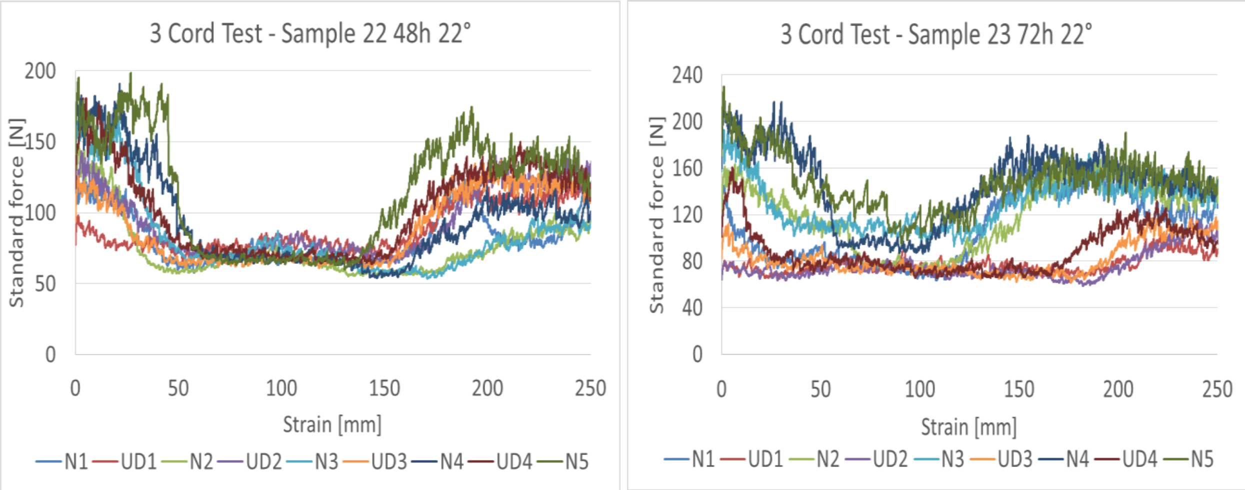

Figure 32 - Evolution of the force for a back layer of 22°

The back layer with the default angle configuration shows the best results for a waiting period of 48 hours. The magnitude of the force is much higher when waiting longer, and for Sample 23, approaching the central cord sets "N4-UD4", the force varies almost 100N.

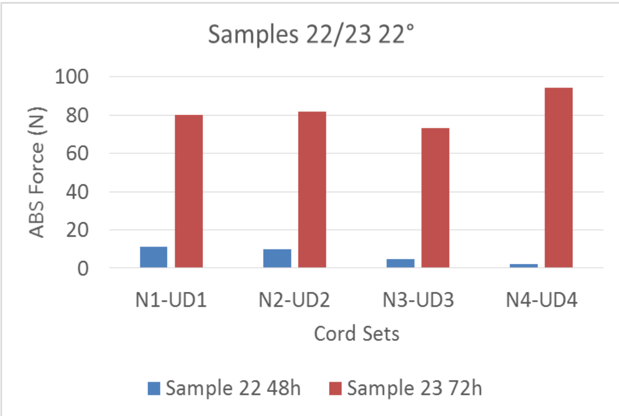

Figure 33 - Evolution of the force towards the centre of the samples 22 and 23

4.1.5.3 Back layer angle of 45° for 48 hours and 72 hours

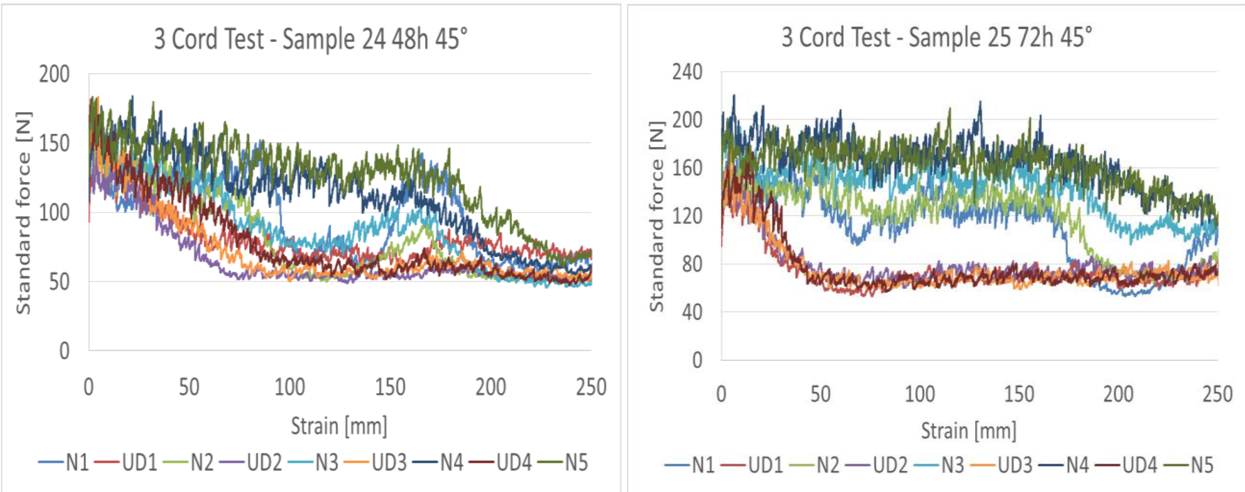

Figure 34 - Evolution of the force for a back layer of 45°

For a back layer with an orientation of 45°, it is clear that for 72 hours and considering the cord sets with normal orientation, the force reaches higher levels, when comparing it after 48 hours.

Regarding the evolution of the force towards the centre of the samples, *Figure 35*, proves once again the increasing expected behaviour, although waiting longer to perform the tests is not effective.

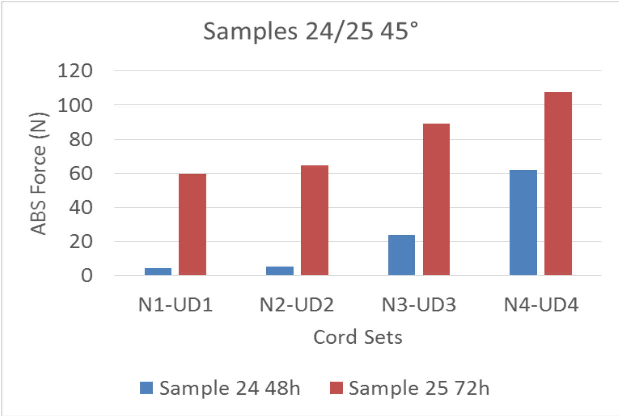

Figure 35- Evolution of the force towards the centre of the samples 24 and 25

4.1.5.4 Back layer angle of 90° for 48 hours and 72 hours

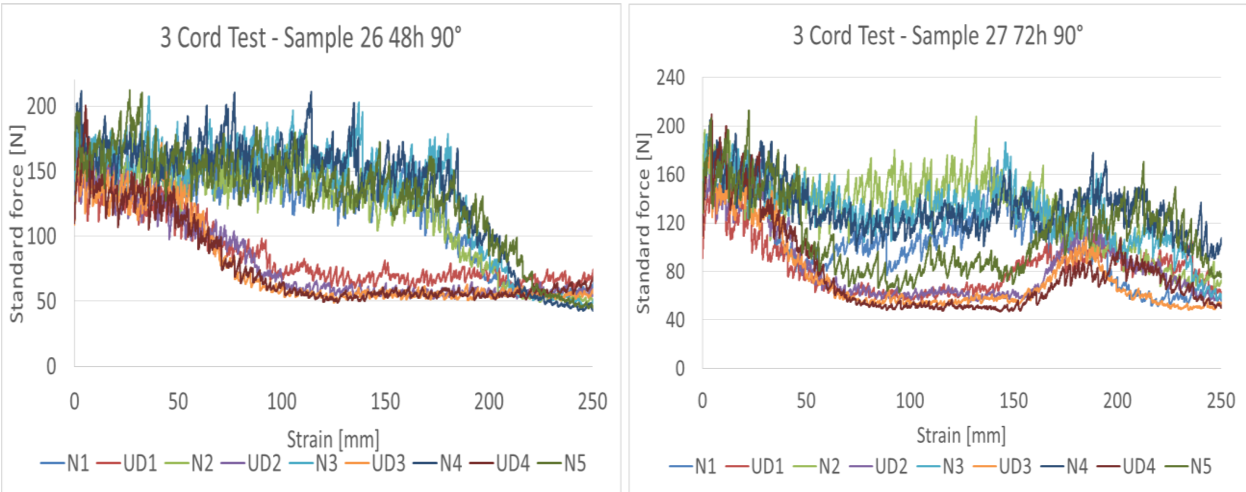

Figure 36 - Evolution of the force for a back layer of 90º

For such back layer configuration, one can realize, at first that the behaviour of the charts show again two levels of force, although the dispersion of it, for the cords sets under a normal orientation, is higher for 72 hours. An interesting detail is related with the fact that due to the very low stiffness of both samples and considering that it naturally tends to bend by itself, as it can be seen on *Figure 38*, around the last 50 mm of strain, the curves tend to change

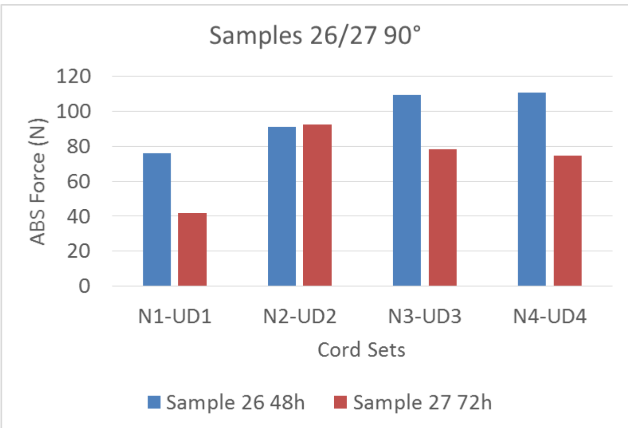

Figure 37 - Evolution of the force towards the centre of the samples 26 and 27

their behaviour. Due to the two levels of force on both cases, there is no possible conclusion, regarding which one is the best suited to perform the tests.

Figure 38 – Natural bending of the sample for a back layer with 90°

4.1.5.5 Conclusions of the Back Layer Angle Effect and waiting time effect

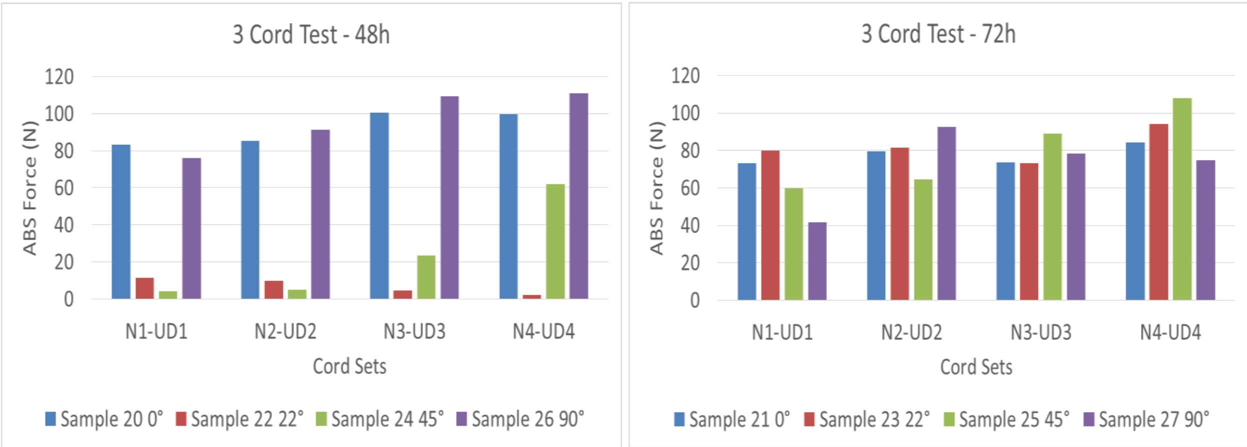

Figure 39 – Evolution of the force throughout the cord sets for all back layer angles and for different waiting times

As it is possible to conclude from *Figure 39*, the overall magnitude of the absolute value of the difference of the force is much higher when performed after 72 hours, and the back layer effect cannot provide a clear conclusion for this scenario.

On the other hand, focusing on the 3 Cord Adhesion Test after waiting for a period of 48 hours, it is easy to verify that for the angles of 0° and 90°, the behaviour is extreme, due to the fact that the stiffness is very high for 0° and low for 90°. Consequently, its levels of force are very high, and the tendency to increase towards the central cord sets is also visible.

Hence, the best choices are those with the back layer with an angle between 22° and 45°. When comparing the evolution of the force for the angle of 45°, although the behavior evolves as expected, the central cord sets reveal a drastic increase. As a conclusion after this study, one can realize that the most appropriate back layer angle is 22° and the test should be performed 48 hours after vulcanization occurs.

4.1.6 3 Cord Adhesion Test – Upgrade Configuration

The reason to implement a new configuration was specified on subchapter 3.1.4.2.

Firstly, to evaluate the efficiency of the new configuration, 3 samples were built and tested after a waiting period of 72 hours. The results presented on *Figure 40*, reveal that there is a new pattern although it does not correspond to the one that should be expected, and shown previously on *Figure 24*. It is evident from these samples, that the cord sets which required more force to be peeled are the ones set under a normal orientation.

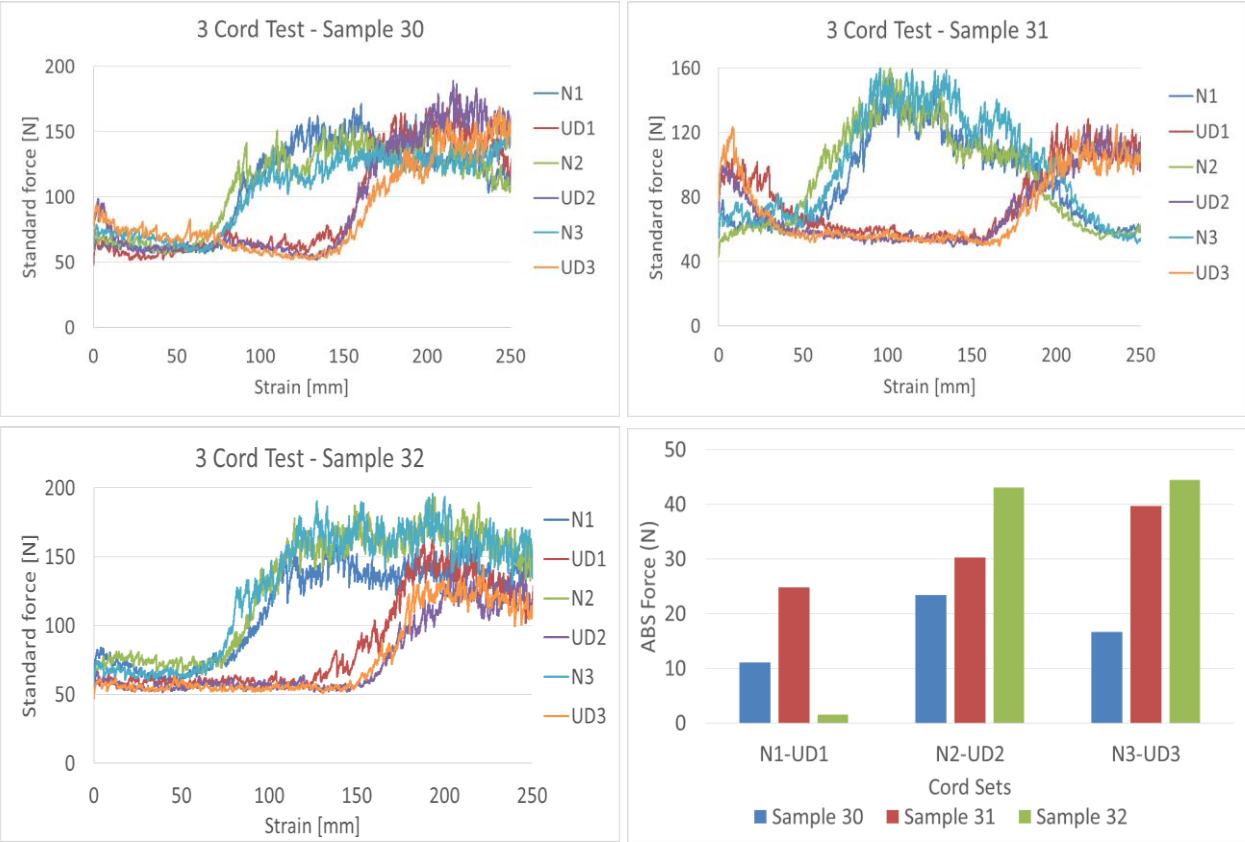

Figure 40 – Illustrations of the 3 Cord Adhesion Test after implementing a new configuration

To understand how the force evolved from the extremes to center of the sample, the same exercise performed on subchapter 4.1.5 was also conducted. The data from which the bar chart on *Figure 40* was created, is present on the Appendix 2.2.

Once again, the evolution of the force goes as expected, however, the magnitude diminished, when comparing to the previous configuration.

In order to check what could be possibly influencing these results, more studies needed to be repeated, and are presented in the next subchapters.

4.1.7 Upgrade Configuration: Influence of the number of cords per cord set

Considering the fact that, with the new configuration, the number of cord sets was reduced, in order to increase the reproducibility of the behaviour obtained for 1 Cord Test, the number of cords per each orientation was maintained at 5.

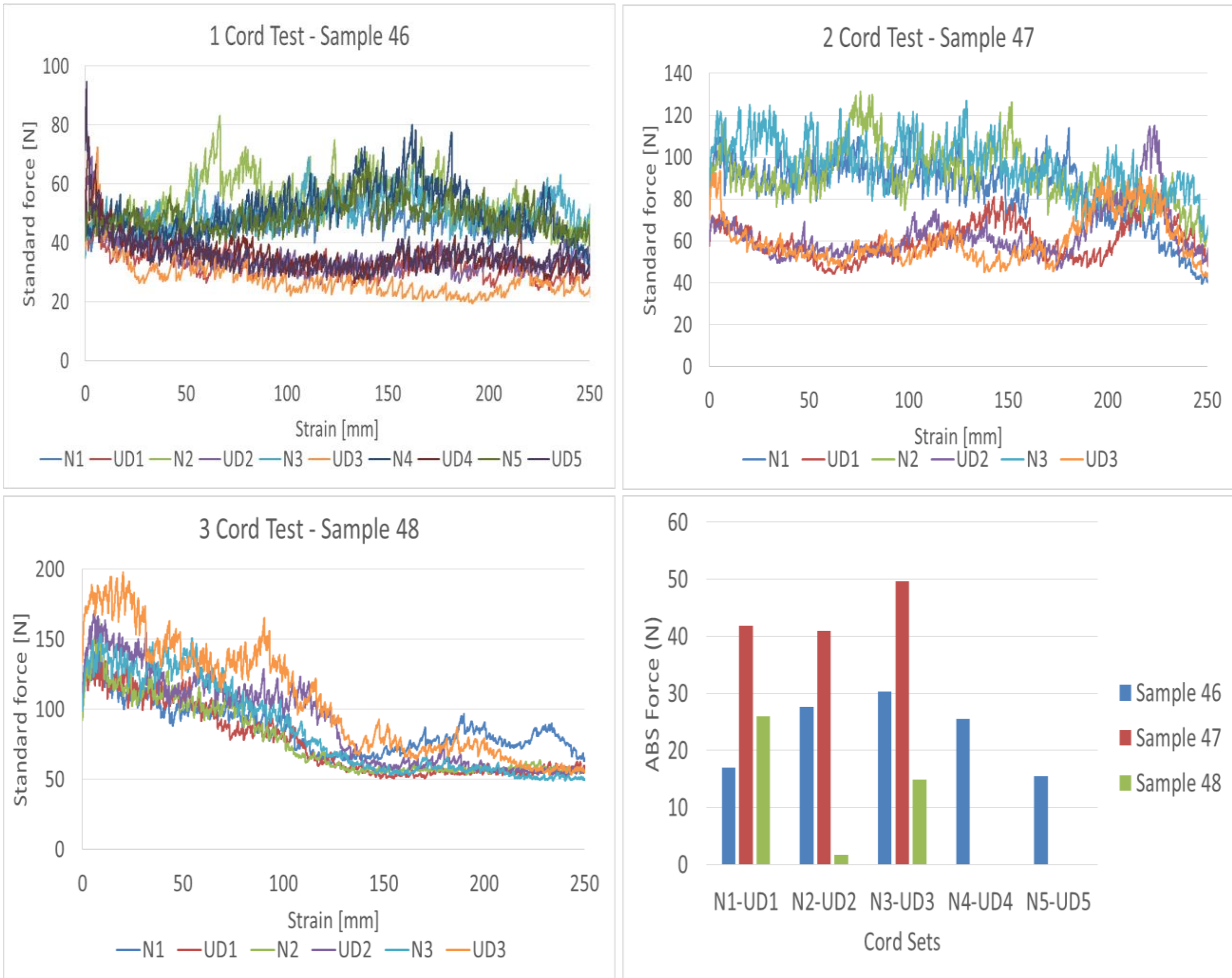

Figure 41 – Illustrations of the evolution of the force for 1,2 and 3 cords per cord set

From *Figure 41*, it is clear, once again, that the best number of cord sets should be 3, not only due to the pattern obtained throughout the sample, and the range of values measured, but also, due to the magnitude of the force when comparing the cord sets under study and presented on the bar chart.

The data from which the bar chart on *Figures 41* was created, is present on the Appendix 2.3.

4.1.8 Upgrade Configuration: Waiting time effect

For a waiting period of 48 hours, the charts presented on *Figure 42* reveal difficulties regarding the analysis of reproducibility. Sample 34 shows a range of force which varies too much when compared to Sample 33. In other words, more samples should be tested.

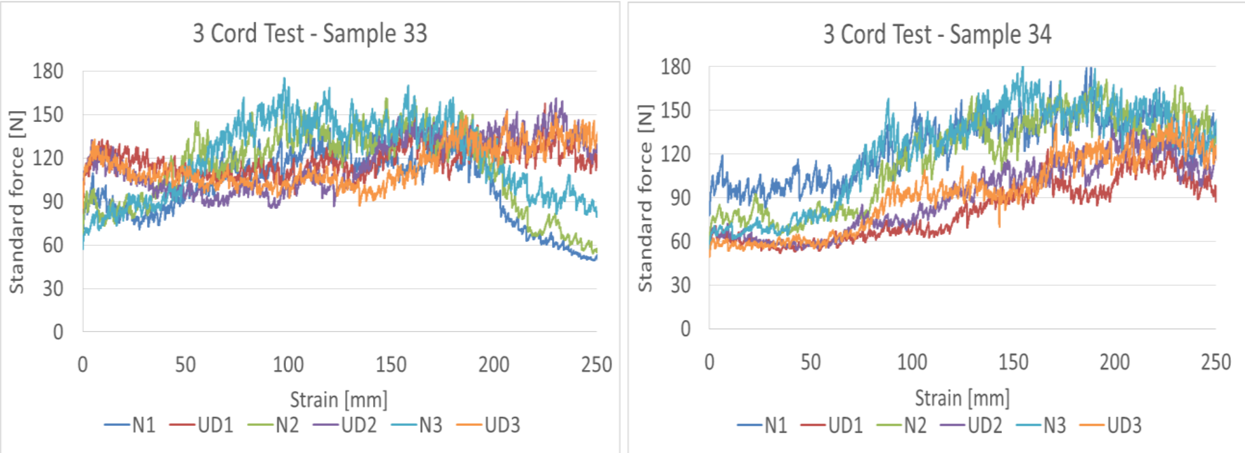

Figure 42 - Evolution of the force for a waiting period of 48 hours

The data used to create the bar chart on *Figure 43* are presented on the Appendix 2.4.

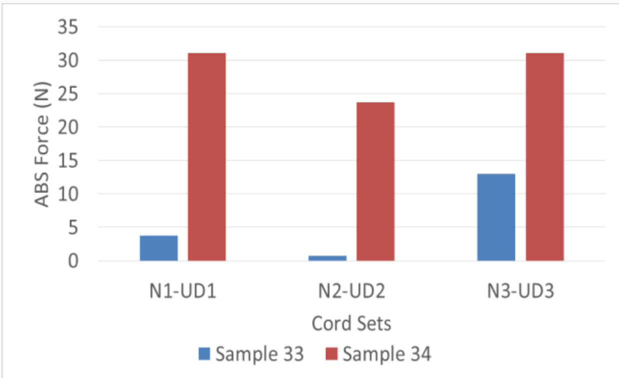

Figure 43 - Evolution of the force towards the centre of the samples 33 and 34

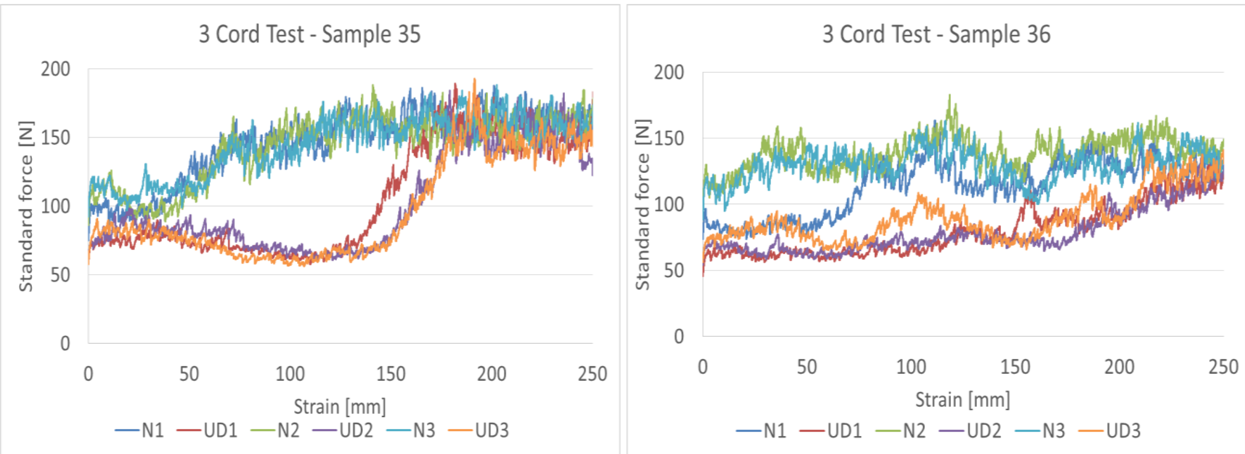

Figure 44 - Evolution of the force for a period of 72 hours

After waiting for a period of 72 hours to perform the test, it is visible that the reproducibility is affected once again. The behaviour of the force varies too much and further studies need to be conducted.

The data used to create the bar chart on *Figure 45* is presented in the Appendix 2.4.

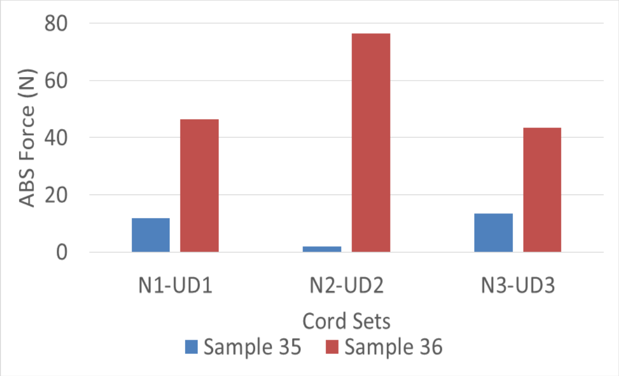

Figure 45 - Evolution of the force towards the centre of the samples 35 and 36

4.2 Oldy Test

4.2.1 Oldy Test: General Information

The Oldy Test was performed to assess the adhesion of rubber to three different textiles: Hybrid, Nylon and Polyester.

Due to confidentiality reasons, the proper nomenclature of the rubber, as well as the nomenclature of the textiles, cannot be presented. Hence, the rubber used is presented “A”, and the textiles cords as “H”, “N” and “P”. Two different types of rubber were used on this test method, and for each textile, the number of adhesion promoters were 2 for the Hybrid, 5 for the Nylon and 2 for the Polyester.

4.2.2 Oldy Test: Hybrid

The hybrid textile was tested with two different adhesion promoters, the first is named as H1 and the second one as H2. On *Table 4*, it is shown information for each of the 8 samples tested for H1. In the Appendix 3.1, it is presented similar information regarding the H2.

During the static test, the input tension imposed for both H1 and H2 was 130N, leading to a regular performance during the dynamic part. Only one specimen broke during the dynamic test, for the reference H2.

Table 4 – Data obtained for the Hybrid compound, reference H1

Textile	***Rubber***		
H1	**A1**		
Sample	**Amplitude (mm)**	**Time (min)**	**Cycles**
1	3	116	35501
2	3	149	45600
3	3	150	45906
4	3	151	46213
5	3	142	43458
6	3	141	43152
7	3	155	47437
8	3	169	51721
	Average	147	44873.57
	Standard Deviation	15.11	4623.86

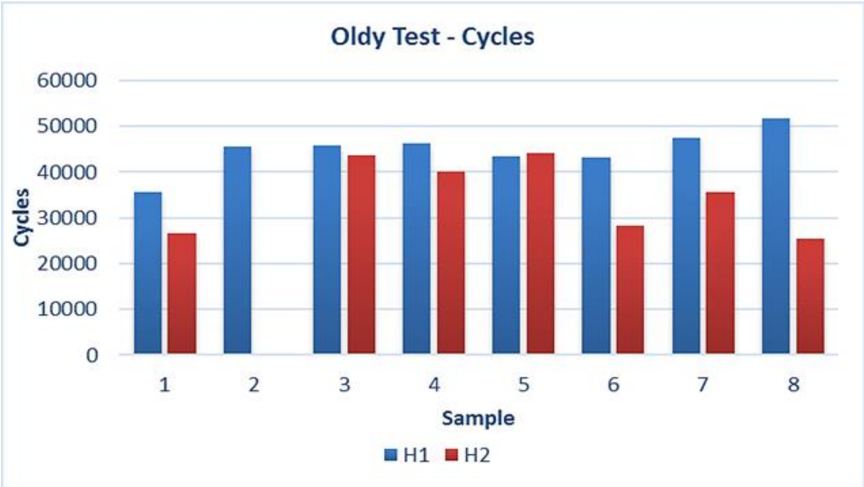

Figure 46 – Cycles reached per sample for the Hybrid adhesion promoters

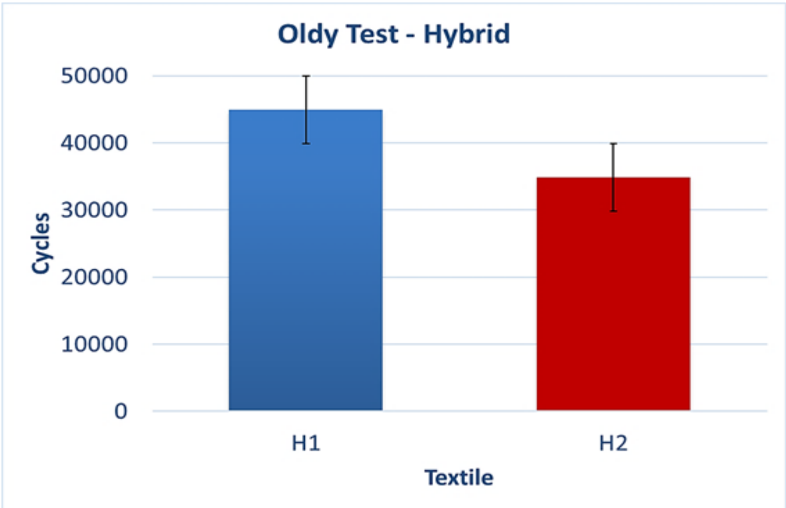

Figure 47 – Standard Deviation of the Hybrid adhesion promoters

From *Figures 46* and *47*, it is visible that the adhesion system between the rubber and the textile cords is better for the reference H1, meaning that this adhesion promoter offers a better performance, leading to a larger number of cycles. Regarding the deviation obtained, it is also visible that for the reference H1, it is smaller and basically half of the value obtained when compared to H2.

4.2.3 Oldy Test: Nylon

The second textile being tested was Nylon, and 5 different adhesion promoters were evaluated: N1, N2, N3, N4 and N5.

On *Table 5*, it is shown information for each of the 8 samples tested for the N1. In the Appendix 3.2, it is presented similar information regarding the 4 other adhesion promoters.

Table 5 - Data obtained for the Nylon, reference N1

Textile	***Rubber***		
N1	**A1**		
Sample	**Amplitude (mm)**	**Time (min)**	**Cycles**
1	3		
2	3		
3	3		
4	3	318	97216
5	3	875	267545
6	3	757	231446
7	3		
8	3	713	218206
	Average	665.63	203603.25
	Standard Deviation	241.68	73926.21

Due to the fact that 4 samples broke in the very beginning of the dynamic test for N1, the reproducibility is largely affected, because the range of cycles varied too much, more specifically, from 97216 to 267545 cycles. One possible reason may be related to the fact that the input tension during the static test, 100N, may have been too high and, as a result, the textile cords were overstressed.

Another reason could be related to the fact that the clamps where the textile cords were attached to, couldn't provide enough stability for the cords throughout the test, causing a premature deterioration of it, making the cords break very fast.

Regarding the remaining 4 Nylon references tested, N2, N3, N4 and N5, more cords broke and the reasons might have been the same as the ones stated previously.

On *Figure 48*, it is presented the performance of all the samples tested for Nylon. It is noticeable that sample 3, from the set of samples N4, reached the highest number of cycles. However, taking into account *Figures 49 and 50*, on average, N5 was the best adhesion promoter, being its deviation inferior to the one obtained for N4.

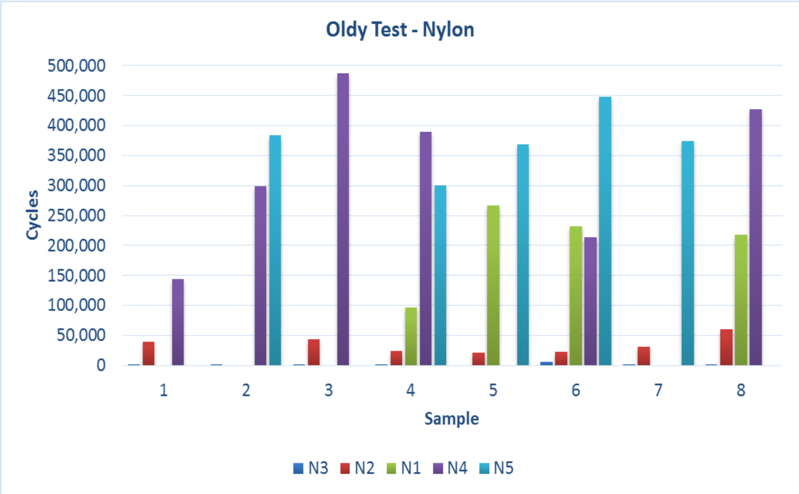

Figure 48 – Cycles reached per sample for the Nylon adhesion promoters

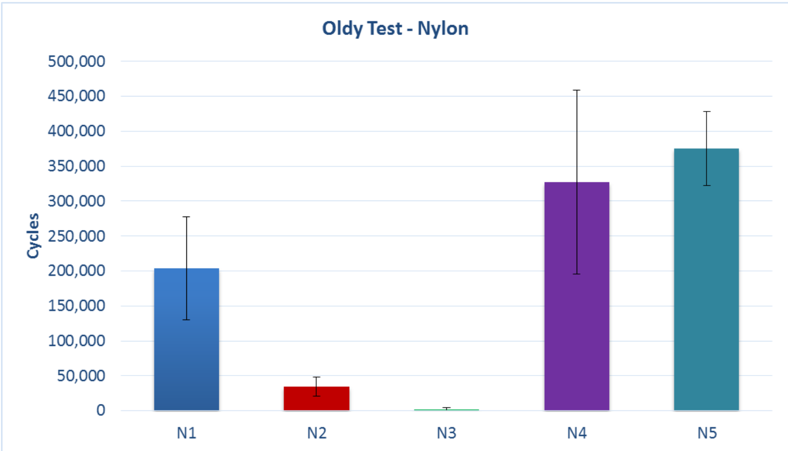

Figure 49 – Standard Deviation of the Nylon adhesion promoters

Focusing on the performance of the textile cords with the reference N3, since there was no adhesion promoter on it, it is possible to realize the proof of concept concerning the adhesion matter. As a result, the number of cycles was the lowest from all 5 adhesion promoters tested.

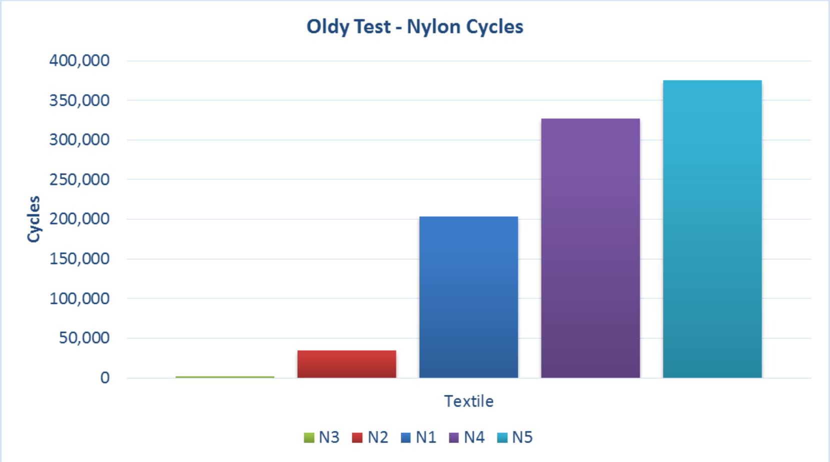

Figure 50 – Rank obtained for all 5 Nylon adhesion promoters

From these results, the need to perform new tests and extend the reproducibility is mandatory, however, due to the lack of time during this internship, it was not possible to repeat the tests.

4.2.4 Oldy Test: Polyester

The last textile under study was Polyester, and two types of adhesion promoters were tested, P1 and P2. In this case, the used rubber is B2 and the amplitude of the test was increased to 3.5 mm. Regarding the static part of the test, the input tension was set at 110N. Only one cord broke, which means that in this case, the force reached during the static test did not overstress the textile cords. On *Table 6*, it is shown information for each of the 8 samples tested for the P1. In the Appendix 3.3, it is presented similar information regarding the adhesion promoter P2.

Table 6 - Data obtained for the Polyester, reference P1

Textile	***Rubber***		
P1	**A2**		
Sample	**Amplitude (mm)**	**Time (min)**	**Cycles**
1	3.5	119	36498
2	3.5	144	44107
3	3.5	135	41360
4	3.5	158	48309
5	3.5		
6	3.5	148	45233
7	3.5	135	41204
8	3.5	185	56519
	Average	146.29	44747.14
	Standard Deviation	20.85	6376.84

For Polyester, and considering *Figure 51*, the performance of both adhesion promoters is similar, being noticeable that there is no significant difference between both adhesion promoters.

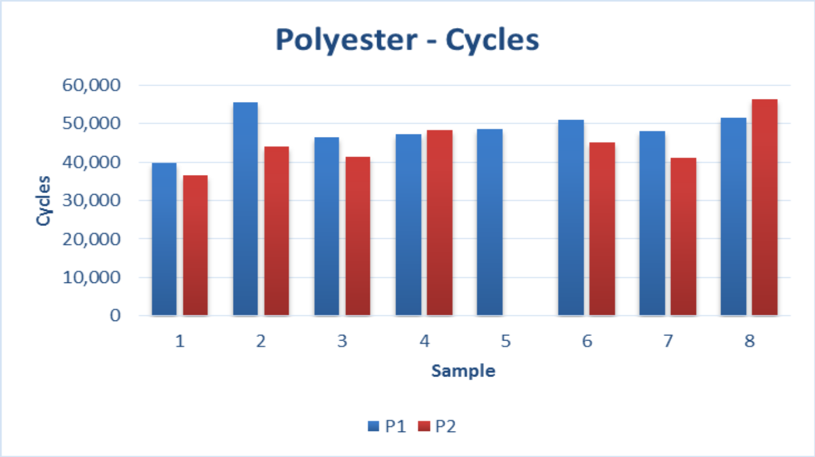

Figure 51 - Cycles reached per sample for the Polyester adhesion promoters

However, statistically, from *Figure 52*, P2 shows better results, meaning that a higher number of cycles was reached, as well as a smaller deviation, comparing to P1.

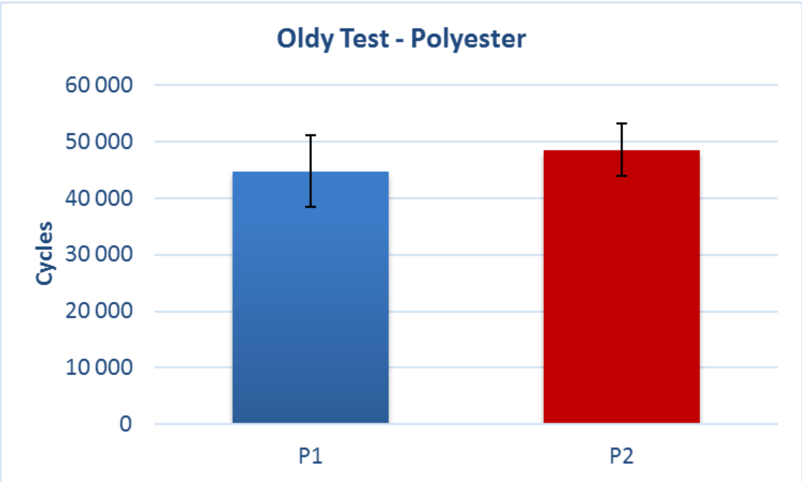

Figure 52 - Standard Deviation for the Polyester adhesion promoters

5 Conclusions

The core of this master thesis was the 3 Cord Adhesion Test. The goal was to go over parameters that could have had an influence on the preliminary results obtained for this test method. Hence, the importance of the symmetry and orientation was implemented and performed on the majority of the samples.

In order to check the influence of the number of cords per cord set, studies were accomplished too, and indeed, there is no reason to change this parameter, having the tests been conducted with 3 steel cords per cord set.

Furthermore, an influencing parameter which showed a relevant impact on the charts obtained, was related to the waiting time between curing and testing of the samples, being 48 hours and 72 hours, the most suitable period of time.

The visual inspection performed in all of the samples confirm a non-uniform behavior of the force throughout the extent of the examination. In other words, it is clear that the level of adhesion between the rubber and the steel cords is not the same on both sides of the samples.

When comparing the back layer angle of the samples and studying the waiting time between curing and testing, the obtained results show a better pattern of force for an angle of 22°, after a waiting period of 48 hours.

Focusing on the Oldy Test, it is verified that from the three different textiles tested, the one providing the best adhesion system between the rubber and the textile cords was Nylon N5, reaching an average of 375136.40 cycles and a standard deviation of ± 52700.85 cycles.

Regarding the Hybrid tested compound, the average number of cycles reached for the best compound, H1, was 44874.00 and the standard deviation was ± 4623.86.

For the Polyester, the best adhesion promoter achieved an average of 48565.00 cycles and the standard deviation was ± 4610.80.

From these results, it is possible to acknowledge the importance of adhesion promoters and how this test, although in a preliminary stage, and in some cases, very time consuming, can lead to relevant results regarding the simulation of dynamic conditions.

6 Project Assessment

6.1 Achieved goals

The goal of this master thesis was to go over two test methods capable to perform both static and dynamic tests, regarding tire reinforcements. For the 3 Cord Adhesion Test, the behavior of the force detected in preliminary tests, showed the need to place the focus on the development of new testing conditions. In other words, it was only possible the performance of the static part of this test method.

The Oldy Test allowed the performance of both static and dynamic tests. Considering that the test method is still under development, for the three textiles tested it was possible to evaluate the adhesion system between the rubber and different adhesion promoters.

6.2 Limitations and Future Work

The limitations encountered throughout this internship were mostly time related. Some suggestions for the 3 Cord Test method are presented on the next subchapters, and these will be crucial for further developments.

Regarding the Oldy Test, due to the fact that some sets of samples were too time consuming, it was impossible to repeat the tests in order to verify the reproducibility, as well as to test new materials.

6.2.1 Zwick Tensile Tester Configuration

The clamps used on the Zwick machine are not the most suitable to conduct the 3 Cord Adhesion Test. The available clamps interfere with the sample, making it bend during the testing. Since there is no possibility to adjust the lower clamp, due to a fixed position, when peeling the cords out, the samples bend and only the steel cords are vertical. On *Figure 53*, it shown the current set up of the clamps.

Suggestion: The need for new clamps is essential in order to minimize friction and to maintain the integrity of the sample. Another suggestion could be to change the configuration of the lower clamp, to a configuration that won't interfere with the sample, allowing the peel of the cords, maintain both the sample and the cords vertically.

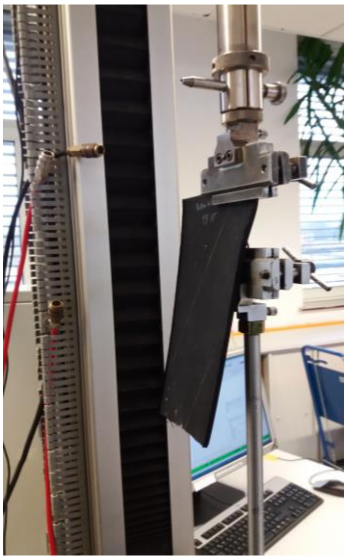

Figure 53 – Current configuration of the clamps

6.2.2 Cutting device to build the samples

Each sample is composed of two rubber sheets (layers) with steel cords inside it. In order to cut them to the appropriate dimensions, the used device was the guillotine available at the laboratory, and shown on *Figure 54*. However, because of the steel cords, the cutting process becomes a possible source of problems, since the device doesn't provide enough stability to cut regular surfaces. Furthermore, since the back layer has an angle of 22°, cutting it is even more difficult.

Suggestion: change for a device such as a hydraulic cutting press machine, present at the laboratory, with an appropriate mould capable to cut the rubber sheets on every side at the same time, *Figure 54*.

Figure 54 – Guillotine (left) and Hydraulic Cutting Press Machine (right)

6.2.3 The mold

The mold plays an important role on the entire building process, considering its inside is where vulcanization occurs. Its configuration ends up shaping the entire sample. One possible reason for the results obtained, may be related to the fact that the mold available at the laboratory is crooked, as it can be perceived from the *Figure 55*.

Figure 55 – Mold's gap detected using a glass surface.

6.3 Final Assessment

Considering the fact that the core of the master thesis had to change in the early weeks of the internship, it was necessary to adapt to a new scenario and gather as much information as possible, to realize all the potential factors which could have been influencing the 3 Cord Adhesion Test Method.

It was necessary to study parameters to which the real influence was never studied before, and with this master thesis, it is clear that, for this test method to be successful, more improvements need to be implemented.

Concerning the difficulties, they were felt due to the lack of technical know-how on both test methods, especially for the Oldy Test, since the test method is still under development. Taking into account the results obtained, it is evident the need to perform more studies so that the reproducibility of the test can be valued, as well as to define the best set conditions for each material.

Despite all the challenges, many goals were achieved and reported regularly, having been quite relevant to Continental.

References

[1] Continental AG, "Facts and figures," [Online]. Available: http://www.continental-tires.com/car/company/about-us/corporate [Accessed September 2016].

[2] Continental AG, “Tyre Basics – Passenger Car Tyres” [Online]. Available http://www.conti-online.com/www/download/banden_nl_nl/algemeen/links/download-area/download/reifengrundlagen_en.pdf [Accessed September 2016]

[3] National Highway Traffic Safety Administration, “The Pneumatic Tire”, 2006.

[4] VERT, "Textile Reinforcement," [Online]. Available: https://www.tut.fi/ms/muo/vert/10_reinforcing_materials/index.htm. [Accessed September 2016].

[5] VERT, "Cotton," [Online]. Available: https://www.tut.fi/ms/muo/vert/10_reinforcing_materials/index.htm. [Accessed September 2016].

[6] VERT, "Steel Reinforcement," [Online]. Available: https://www.tut.fi/ms/muo/vert/10_reinforcing_materials/index.htm. [Accessed September 2016].

[7] T. Kramer, "Basics of Reinforcements," in *TireAcademy*.

[8] B. Crowther, “*Handbook of Rubber Bonding*”. Shawbury: RAPRA Technology LTD, 2001.

[9] W. Fulton, "Steel Tire Cord-Rubber Adhesion, Including the Contribution of Cobalt," *Rubber Chem Technol,* 2005.

[10] Adhesion of brass plated steel cords to natural rubber: “Dynamic and statistical study of adhesion failure,” 2013

[11] M. Jamshidi, F. Afshar, B. Shamayeli, “Evaluation of cord/rubber adhesion by a new fatigue test method”, 2006.

[12] K. Mitsuhashi, "Methods of dynamic adhesion testing," *Nippon Gomu Kyokaishi,* 1981.

[13] K. Mitsuhashi, "Dynamic adhesion fatigue tests II," *Nippon Gomu Kyokaishi,* 1981.

[14] Zwick Roell, "Zwick Roell Website," [Online]. Available: http://www.zwick.co.uk/en/products/static-materials-testing-machines/testingmachines-from-5-kn-to-250-kn/allround-line-materials-testing-machines.html. [Accessed September 2016].

[15] MTS, "MTS High-Force Servohydraulic Test Systems," [Online]. Available: https://www.mts.com/ucm/groups/public/documents/library/dev_004848.pdf. [Accessed September 2016].

[16] N. Goldfinger, S. Sostmann, “New insights into the effects of dynamic load on the fiber/matrix interface”

[17] N. Goldfinger, S. Sostmann, “Consequences of dynamic load for the strength of the fiber/matrix-interface”

Appendix 1 – Oldy Test

Appendix 1.1 - Sample Preparation

- Ruler, Scissors.
- Use gloves to prevent the rubber from getting dirt.
- Clean the ruler with alcohol throughout the entire procedure.
- Cut the edges of the rubber surface to get a straight line/surface.
- Thickness: 1mm.
- The primary goal is to obtain a rubber stripe as the one presented in the following picture

Figure 56 – The length of the stripe varies according to the rubber sheets provided

- To do that, insert the protective film on top of the rubber to prevent it from getting dirt.

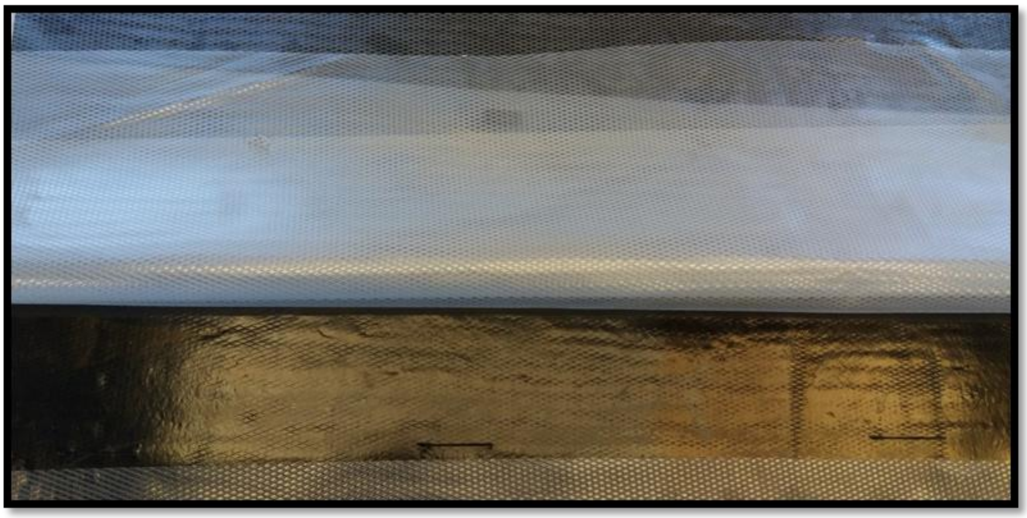

Figure 57 – Protective film on both sides of the rubber sheet. To cut the stripes, minimize the contact between the ruler and the rubber

- Cut 3 or 4 stripes.
- Regarding the textile cords:

- <u>Dark cords:</u> 8 samples with RFL system (adhesion promoter).
- <u>Light cords:</u> 8 samples without the RFL system.
- <u>Length of the cords:</u> around 80 cm.

Figure 58 – Textile cord with RFL system (left) and without (right)

- The next step is to roll the textile cord inside the rubber stripes. To do that, make sure to follow the next picture and keep the distance of 20cm to the right of the rubber sample.

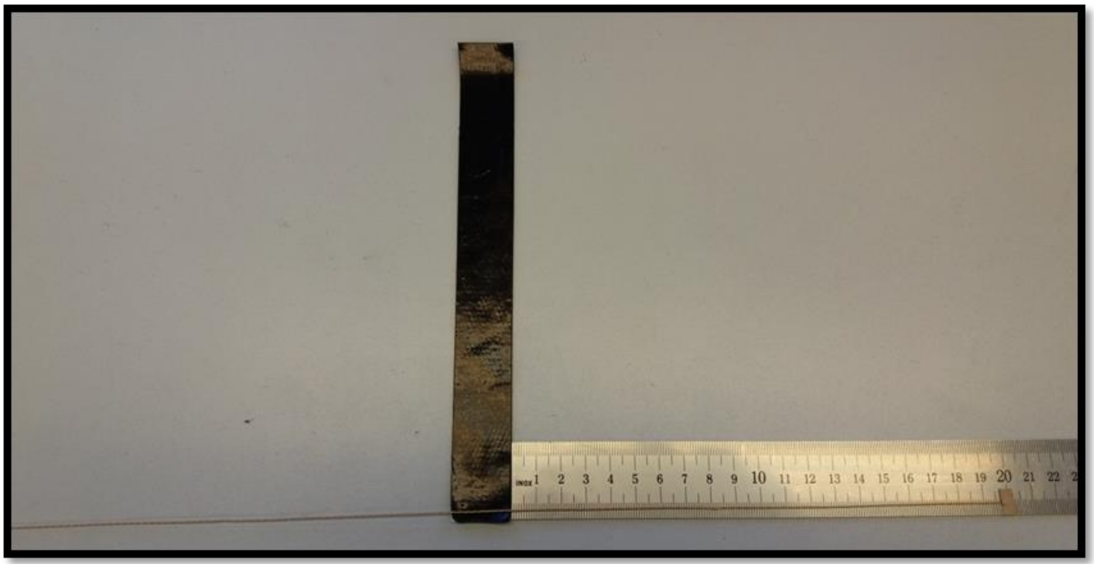

Figure 59 – Regular layout of the cord and the rubber

- Weigh the sample: it must be 5.25g (±0.02 g). At first, for each sample, it's necessary to tare the cord, before it is rolled inside the rubber.

Figure 60 – To weigh the sample, make sure that the entire cord is on the plate

- Get an appropriate foil to put the samples on.
- Cut one wire to put in the border of the heat press machine, to prevent the mold from moving during vulcanization.
- Card board to put the samples on.
- In the heat press, make sure that the mold doesn't get too cold. If necessary, pre-heat or wait until the machine cools down to the appropriate temperature.
- When inserting the samples inside the mold, the bottom mold part is recognizable due to the existence of two larger holes where the cords are introduced.
- Make sure to use the clips available to fix them and prevent the sample from moving during vulcanization.
- Insert the upper mold part.
- Insert the weights in each cord sample.
- Start the machine using the buttons on the lower part of the surface.
- After vulcanization remove the samples to the card board.
- Number the samples exactly as they were taken from the heat press.

Appendix 1.2 - Sample Cleaning

- Remove all the extra rubber from the samples.
- Make sure that the cord is free to move and there´s no rubber attached to the ends of the rubber sample. If not carefully verified, it will interfere with the following tests.

Appendix 2 – 3 Cord Test Data

Appendix 2.1

Table 7 – Range of data considered to evaluate the force between cord sets for Sample 20

Angle: 0°

48h										
Sample 20		**N1**	**N2**	**N3**	**N4**	**N5**	**UD4**	**UD3**	**UD2**	**UD1**
	Considered Range (mm)	**160-230**	**150-230**	**130-210**	**150-230**	**160-240**	**30-100**	**50-120**	**50-120**	**50-120**
	Force(N)	178.59	171.11	188.75	180.04	164.83	80.31	88.35	86.02	95.43
	Average Force	**N**	**179.6**				**U D**	**87.5**		
		N1-UD1	**N2-UD2**	**N3-UD3**	**N4-UD4**					
	ABS(Δ)	83.16	85.09	100.4	99.73					

Table 8 - Range of data considered to evaluate the force between cord sets for Sample 21

Angle: 0°

72h										
Sample 21		**N1**	**N2**	**N3**	**N4**	**N5**	**UD4**	**UD3**	**UD2**	**UD1**
	Considered Range (mm)	**150-200**	**100-200**	**100-200**	**100-200**	**100-200**	**100-200**	**100-200**	**100-200**	**150-200**
	Force(N)	96.57	96.55	102.95	89.3	94.85	173.52	176.73	175.99	169.9
	Average Force	**N**	**96.3**				**U D**	**174.0**		
		N1-UD1	**N2-UD2**	**N3-UD3**	**N4-UD4**					
	ABS(Δ)	73.33	79.44	73.78	84.22					

Table 9 Range of data considered to evaluate the force between cord sets for Sample 22

Angle: 22°										
48h										
Sample 22		**N1**	**N2**	**N3**	**N4**	**N5**	**UD4**	**UD3**	**UD2**	**UD1**
	Considered Range (mm)	**70-150**	**70-150**	**70-150**	**70-150**	**70-130**	**70-150**	**70-150**	**70-150**	**70-150**
	Force(N)	68.85	67.18	71.88	69.11	67.9	71.21	67.15	77.07	80.06
	Average Force	**N**	**69.3**				**U D**	**73.9**		
		N1-UD1	**N2-UD2**	**N3-UD3**	**N4-UD4**					
	ABS(Δ)	11.21	9.89	4.73	2.1					

Table 10 - Range of data considered to evaluate the force between cord sets for Sample 23

Angle: 22°										
72h										
Sample 23		**N1**	**N2**	**N3**	**N4**	**N5**	**UD4**	**UD3**	**UD2**	**UD1**
	Considered Range (mm)	**150-210**	**160-220**	**150-230**	**140-210**	**130-200**	**70-150**	**70-150**	**70-150**	**70-150**
	Force(N)	156.64	153.95	147.66	168.69	156.49	74.58	74.43	72.38	76.66
	Average Force	**N**	**156.7**				**U D**	**74.5**		
		N1-UD1	**N2-UD2**	**N3-UD3**	**N4-UD4**					
	ABS(Δ)	79.98	81.57	73.23	94.11					

Table 11 - Range of data considered to evaluate the force between cord sets for Sample 24

Angle: 45°

48h										
Sample 24		**N1**	**N2**	**N3**	**N4**	**N5**	**UD4**	**UD3**	**UD2**	**UD1**
	Considered Range (mm)	**95-155**	**90-150**	**80-140**	**80-140**	**100-160**	**100-160**	**100-160**	**100-160**	**100-160**
	Force(N)	74.58	60.42	81.93	125.89	137.16	63.96	58.29	55.43	70.47
	Average Force	**N**	**85.7**				**U D**	**62.0**		
		N1-UD1	**N2-UD2**	**N3-UD3**	**N4-UD4**					
	ABS(Δ)	4.11	4.99	23.64	61.93					

Table 12 - Range of data considered to evaluate the force between cord sets for Sample 25

Angle: 45°

72h										
Sample 25		**N1**	**N2**	**N3**	**N4**	**N5**	**UD4**	**UD3**	**UD2**	**UD1**
	Considered Range (mm)	**100-170**	**100-170**	**50-150**	**50-150**	**50-150**	**100-200**	**100-200**	**100-200**	**100-200**
	Force(N)	131.78	139.1	158.04	177.95	174.54	70.16	69.03	74.67	72.13
	Average Force	**N**	**151.7**				**U D**	**71.5**		
		N1-UD1	**N2-UD2**	**N3-UD3**	**N4-UD4**					
	ABS(Δ)	59.65	64.43	89.01	107.79					

Table 13 - Range of data considered to evaluate the force between cord sets for Sample 26

Angle: 90°

48h										
Sample 26		**N1**	**N2**	**N3**	**N4**	**N5**	**UD4**	**UD3**	**UD2**	**UD1**
	Considered Range (mm)	**60-130**	**60-130**	**60-130**	**60-130**	**60-130**	**100-170**	**100-170**	**100-170**	**100-170**
	Force(N)	148.74	152.36	166.25	167.39	150.55	56.57	56.85	61.25	72.68
	Average Force	**N**	**158.7**				**U D**	**61.8**		
		N1-UD1	**N2-UD2**	**N3-UD3**	**N4-UD4**					
	ABS(Δ)	76.06	91.11	109.4	110.82					

Table 14 - Range of data considered to evaluate the force between cord sets for Sample 27

Angle: 90°

72h										
Sample 27		**N1**	**N2**	**N3**	**N4**	**N5**	**UD4**	**UD3**	**UD2**	**UD1**
	Considered Range (mm)	**50-120**	**50-120**	**70-140**	**60-180**	**170-230**	**70-140**	**70-140**	**70-140**	**60-130**
	Force(N)	105.76	155.88	135.05	126.8	130.99	52.18	56.55	63.31	64.02
	Average Force	**N**	**130.9**				**U D**	**59.0**		
		N1-UD1	**N2-UD2**	**N3-UD3**	**N4-UD4**					
	ABS(Δ)	41.74	92.57	78.5	74.62					

Appendix 2.2

Table 15 - Range of data considered to evaluate the force between cord sets for Sample 30

72h

Sample 30		N1	N2	N3	UD3	UD2	UD1
	Considered Range (mm)	**130-230**	**130-200**	**150-230**	**205-245**	**205-245**	**180-230**
	Force(N)	143.9	141.17	133.14	149.79	164.61	155.01
	Average Force	**N**	**139.4**		**U D**	**156.5**	
		N1-UD1	**N2-UD2**	**N3-UD3**			
	ABS(Δ)	11.11	23.44	16.65			

Table 16 - Range of data considered to evaluate the force between cord sets for Sample 31

72h

Sample 31		N1	N2	N3	UD3	UD2	UD1
	Considered Range (mm)	**90-130**	**90-130**	**90-140**	**200-240**	**210-249**	**200-240**
	Force(N)	136.24	142.11	147.58	107.89	111.81	111.42
	Average Force	**N**	**142.0**		**U D**	**110.4**	
		N1-UD1	**N2-UD2**	**N3-UD3**			
	ABS(Δ)	24.82	30.3	39.69			

Table 17 - Range of data considered to evaluate the force between cord sets for Sample 32

72h

Sample 32		N1	N2	N3	UD3	UD2	UD1
	Considered Range (mm)						
	Force(N)	143.84	167.77	170.88	126.43	124.66	145.42
	Average Force	**N**	**160.8**		**U D**	**132.2**	
		N1-UD1	**N2-UD2**	**N3-UD3**			
	ABS(Δ)	1.58	43.11	44.45			

Appendix 2.3

Table 18 - Range of data considered to evaluate the force between cord sets for Sample 46

1 Cord Test

48h											
Sample 46		**N1**	**N2**	**N3**	**N4**	**N5**	**UD5**	UD4	**UD3**	**UD2**	**UD1**
	Considered Range (mm)	**130-200**	**100-170**	**120-200**	**120-200**	**150-220**	**150-220**	**150-210**	**100-200**	**100-200**	**100-200**
	Force(N)	50.87	62.21	55.48	61.73	52.88	37.4	36.18	25.18	34.54	33.94
	Average Force	**N**	**56.6**				**U D**	**33.4**			
		N1-UD1	**N2-UD2**	**N3-UD3**	**N4-UD4**	**N5-UD5**					
	ABS(Δ)	16.93	27.67	30.3	25.55	15.48					

Table 19 - Range of data considered to evaluate the force between cord sets for Sample 47

2 Cord Test

48h							
Sample 47		**N1**	**N2**	**N3**	**UD3**	**UD2**	**UD1**
	Considered Range (mm)	**50-150**	**100-170**	**50-150**	**70-170**	**70-170**	**160-200**
	Force(N)	96.92	102.7	106.47	56.89	61.82	55.04
	Average Force	**N**	**102.0**		**U D**	**57.9**	
		N1-UD1	**N2-UD2**	**N3-UD3**			
	ABS(Δ)	41.88	40.88	49.58			

Table 20 - Range of data considered to evaluate the force between cord sets for Sample 48

3 Cord Test

48h							
Sample 48		**N1**	**N2**	**N3**	**UD3**	**UD2**	**UD1**
	Considered Range (mm)	**170-240**	**150-240**	**150-240**	**150-240**	**150-240**	**150-240**
	Force(N)	82.3	58.2	56.92	71.78	59.95	56.31
	Average Force	**N**	**65.8**		**U D**	**62.7**	
		N1-UD1	**N2-UD2**	**N3-UD3**			
	ABS(Δ)	25.99	1.75	14.86			

Appendix 2.4

Table 21 - Range of data considered to evaluate the force between cord sets for Sample 33

48h

Sample 33							
		N1	**N2**	**N3**	**UD3**	**UD2**	**UD1**
	Considered Range (mm)	**100-150**	**100-150**	**100-150**	**180-230**	**150-200**	**150-200**
	Force(N)	126.66	139.71	146.93	133.96	138.93	130.39
	Average Force	**N**	**137.8**		**U D**	**134.4**	
		N1-UD1	**N2-UD2**	**N3-UD3**			
	ABS(Δ)	3.73	0.78	12.97			

Table 22 - Range of data considered to evaluate the force between cord sets for Sample 34

48h

Sample 34							
		N1	**N2**	**N3**	**UD3**	**UD2**	**UD1**
	Considered Range (mm)	**120-180**	**150-210**	**130-200**	**170-230**	**195-230**	**200-230**
	Force(N)	147.92	153.11	156.98	125.92	129.45	116.79
	Average Force	**N**	**152.7**		**U D**	**124.1**	
		N1-UD1	**N2-UD2**	**N3-UD3**			
	ABS(Δ)	31.13	23.66	31.06			

Table 23 - Range of data considered to evaluate the force between cord sets for Sample 35

72h

Sample 35		**N1**	**N2**	**N3**	**UD3**	**UD2**	**UD1**
	Considered Range (mm)	**150-230**	**150-230**	**150-230**	**180-240**	**180-240**	**170-240**
	Force(N)	171.7	160.22	164.8	151.31	158.18	159.79
	Average Force	**N**	**165.6**		**U D**	**156.4**	
		N1-UD1	**N2-UD2**	**N3-UD3**			
	ABS(Δ)	11.91	2.04	13.49			

Table 24 - Range of data considered to evaluate the force between cord sets for Sample 36

72h

Sample 36		**N1**	**N2**	**N3**	**UD3**	**UD2**	**UD1**
	Considered Range (mm)	**170-240**	**170-240**	**170-240**	**200-249**	**100-150**	**210-249**
	Force(N)	136.9	151.56	137.07	128.21	75.25	118.29
	Average Force	**N**	**141.8**		**U D**	**107.3**	
		N1-UD1	**N2-UD2**	**N3-UD3**			
	ABS(Δ)	18.61	76.31	8.86			

Appendix 3 – Oldy Test Data

Appendix 3.1: Hybrid

Table 25 - Data obtained for the Hybrid, reference H2

Textile	***Rubber***		
H2	**A1**		
Sample	**Amplitude (mm)**	**Time (min)**	**Cycles**
1	3	87	26625.00
2	3		
3	3	143	43762.93
4	3	131	40090.52
5	3	144	44068.97
6	3	92	28155.17
7	3	116	35500.00
8	3	83	25400.86
	Average	114	34800.49
	Standard Deviation	26.48	8104.07

Appendix 3.2: Nylon

Table 26 - Data obtained for the Nylon, reference N2

Textile	***Rubber***		
N2	**A1**		
Sample	**Amplitude (mm)**	**Time (min)**	**Cycles**
1	3	127	39000
2	3		
3	3	142	43500
4	3	79	24200
5	3	71	21700
6	3	74	22600
7	3	101	30800
8	3	197	60100
	Average	113.00	34557.14
	Standard Deviation	45.97	14034.58

Table 27 - Data obtained for the Nylon, reference N3

Textile	***Rubber***		
N3	**A1**		
Sample	**Amplitude (mm)**	**Time (min)**	**Cycles**
1	3	5	1425
2	3	3	839
3	3	7	2005
4	3	7	2012
5	3		
6	3	20	6131
7	3	5	1560
8	3	5	1555
	Average	7.25	2218.14
	Standard Deviation	5.79	1770.24

Table 28 - Data obtained for the Nylon, reference N4

Textile	***Rubber***		
N4	**A1**		
Sample	**Amplitude (mm)**	**Time (min)**	**Cycles**
1	3	471	144052
2	3	979	299486
3	3	1592	486848
4	3	1274	389754
5	3		
6	3	698	213443
7	3		
8	3	1398	427504
	Average	1068.54	326847.83
	Standard Deviation	430.53	131690.96

Table 29 - Data obtained for the Nylon, reference N5

Textile	***Rubber***		
N5	**A1**		
Sample	**Amplitude (mm)**	**Time (min)**	**Cycles**
1	3		
2	3	1257	384514
3	3		
4	3	980	299913
5	3	1204	368150
6	3	1465	448035
7	3	1226	375070
8	3		
	Average	1226.41	375136.40
	Standard Deviation	172.29	52700.85

Appendix 3.3: Polyester

Table 30 - Data obtained for the Polyester, reference P2

Textile	***Rubber***		
P2	**A2**		
Sample	**Amplitude (mm)**	**Time (min)**	**Cycles**
1	3.5	130	39744
2	3.5	182	55538
3	3.5	152	46470
4	3.5	154	47191
5	3.5	159	48625
6	3.5	167	51017
7	3.5	158	48213
8	3.5	169	51722
	Average	158.77	48565.00
	Standard Deviation	15.07	4610.80